MARINE GEOLOGY

INTERNATIONAL JOURNAL OF MARINE GEOLOGY, GEOCHEMISTRY AND GEOPHYSICS

Marine Geology 138 (1997) 273–301

Characteristics of seamounts near Hawaii as viewed by *GLORIA*

Nathan T. Bridges [1]

Department of Geosciences, University of Massachusetts, Amherst, MA 01003, USA

Received 8 March 1996; accepted 19 November 1996

ELSEVIER

MARINE GEOLOGY

Scope of the journal

Marine Geology is an international medium for the publication of original studies and comprehensive reviews in the field of Marine Geology, Geochemistry and Geophysics. The editors endeavour to maintain a high scientific level and it is hoped that with its international coverage the journal will contribute to the sound development of this field.
A *letter section* is provided as a publication outlet for short papers which require *rapid* publication.

Publication information

Marine Geology (ISSN 0025-3227). For 1997 volumes 137-144 are scheduled for publication. Subscription prices are available upon request from the publisher. Subscriptions are accepted on a prepaid basis only and are entered on a calendar year basis. Issues are sent by surface mail except to the following countries where air delivery via SAL is ensured: Argentina, Australia, Brazil, Canada, Hong Kong, India, Israel, Japan, Malaysia, Mexico, New Zealand, Pakistan, PR China, Singapore, South Africa, South Korea, Taiwan, Thailand, USA. For all other countries airmail rates are available upon request. Claims for missing issues must be made within six months of our publication (mailing) date. For orders, claims, product enquiries (no manuscript enquiries) please contact the Customer Support Department at the Regional Sales Office nearest to you:

New York, Elsevier Science, P.O. Box 945, New York, NY 10159-0945, USA. Tel: (+1) 212-633-3730, [Toll Free number for North American Customers: 1-888-4ES-INFO (437-4636)], Fax (+1) 212-633-3680, E-mail: usinfo-f@elsevier.com
Amsterdam, Elsevier Science, P.O. Box 211, 1000 AE Amsterdam, The Netherlands. Tel: (+31) 20-485-3757, Fax: (+31) 20-485-3432, E-mail: nlinfo-f@elsevier.nl
Tokyo, Elsevier Science, 9-15, Higashi-Azabu 1-chome, Minato-ku, Tokyo 106, Japan. Tel. (+81) 3-5561-5033, Fax: (+81) 3-5561-5047, E-mail: kyf04035@niftyserve.or.jp
Singapore, Elsevier Science, No. 1 Temasek Avenue, #17-01 Millenia Tower, Singapore 039192. Tel: (+65) 434-3727, Fax: (+65) 337-2230, E-mail: asiainfo@elsevier.com.sg

US mailing notice — *Marine Geology* (ISSN 0025-3227) is published monthly by Elsevier Science, (Molenwerf 1, Postbus 211, 1000 AE Amsterdam). Annual subscription price in the USA US$2316 (US$ price valid in North, Central and South America only), including air speed delivery. Periodicals postage paid at Jamaica, NY 11431. USA POSTMASTERS: Send address changes to *Marine Geology*, Publications Expediting, Inc., 200 Meacham Avenue, Elmont, NY 11003. Airfreight and mailing in the USA by Publications Expediting.

 0025-3227/97/$17.00

♾ The paper used in this publication meets the requirements of ANSI/NISO Z39.48-1992. (Permanence of Paper).
PRINTED IN THE NETHERLANDS

ELSEVIER

Marine Geology 138 (1997) 273–301

MARINE GEOLOGY
INTERNATIONAL JOURNAL OF MARINE GEOLOGY, GEOCHEMISTRY AND GEOPHYSICS

Characteristics of seamounts near Hawaii as viewed by *GLORIA*

Nathan T. Bridges [1]

Department of Geosciences, University of Massachusetts, Amherst, MA 01003, USA

Received 8 March 1996; accepted 19 November 1996

Abstract

Using images and data acquired from the *GLORIA* sonar system, 390 seamounts within the U.S. Hawaiian Exclusive Economic Zone (HEEZ) off Hawaii have been studied. Their diameters range from 1 to 57 km, with most less than 15 km. Seamount abundance increases exponentially with decreasing size. The areal density of observed seamounts having diameters greater than 1 km is $182/10^6$ km^2. The theoretical abundance of seamounts of all sizes normalized to a unit area is $(309 \pm 17)/10^6$ km^2, about an order of magnitude less than other surveyed areas of the Pacific. This may reflect a lower abundance of Cretaceous seamounts in this region, the covering of small seamounts by sediment, or discrepancies from the use of different data sets to derive the abundance statistics. The seamounts have morphologies ranging from steep-sided, flat-topped structures to cones to more amorphous structures; they are similar to volcanoes found elsewhere on the seafloor. A suite of secondary features associated with the seamounts includes summit craters, summit mounds, coalesced boundaries, landslides, and graben. Several seamount chains are aligned parallel to Cretaceous fracture zones, consistent with an origin close to the ancestral East Pacific Rise. Others are aligned parallel to the Necker Ridge, suggesting that they formed contemporaneously with Necker in the plate interior. This observation, together with high abundances of seamounts where other intraplate igneous processes have occurred, suggests some seamounts formed since leaving the spreading center. © 1997 Elsevier Science B.V.

Keywords: Seamounts; Hawaii; *GLORIA* sonar; North Arch lava flow; Musicians seamounts

1. Introduction

The oceanic crust surrounding the Hawaiian Islands was created at the East Pacific Rise (EPR) approximately 70–130 Myr ago (Atwater and Severinghaus, 1988). Relict tectonic features from the time of spreading include the Murray and Molokai Fracture Zones (FZ's) and the seafloor fabric perpendicular to them (Fig. 1). Other tectonic features of enigmatic origin and age include the Necker and other unnamed ridges, which trend obliquely to the seafloor fabric, indicating that they probably formed in the Pacific Plate interior at a later time. Hawaiian hotspot volcanism and the resulting islands and their products have also modified the seafloor. The region is dominated by the Hawaiian Ridge, a string of subaerial and subaqueous volcanoes erupted from the Hawaiian hotspot and carried successively northwest by movement of the Pacific Plate (Clague and Dalrymple, 1989). The load of the Ridge has

[1]Present address: Jet Propulsion Laboratory, MS 230–235, 4800 Oalc Grove Dr., Pasadena, CA 91109, USA. Tel.: (818) 393-7799; fax: (818) 393-1227;
e-mail: nathan.bridges@jpl.nasa.gov.

PII S0025-3227(96)00114-4

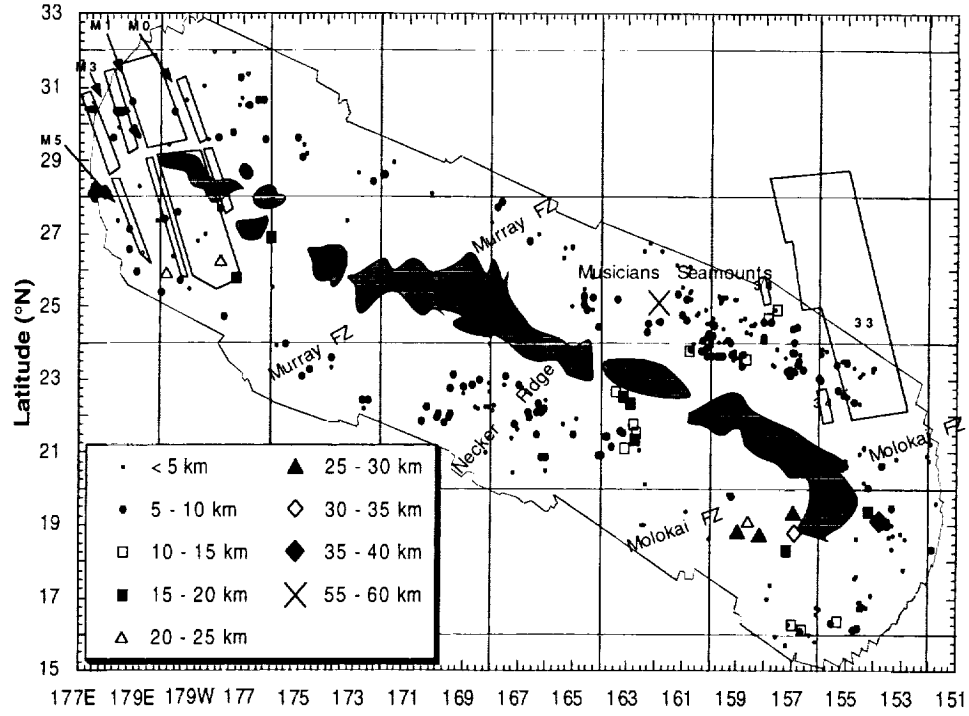
M1
M0
M3
M5
Murray FZ
Musicians Seamounts
Murray FZ
Necker Ridge
Molokai FZ
Molokai FZ
< 5 km
5 - 10 km
10 - 15 km
15 - 20 km
20 - 25 km
25 - 30 km
30 - 35 km
35 - 40 km
55 - 60 km
Latitude (°N)
Longitude (°)
177E 179E 179W 177 175 173 171 169 167 165 163 161 159 157 155 153 151
33 31 29 27 25 23 21 19 17 15

(a)

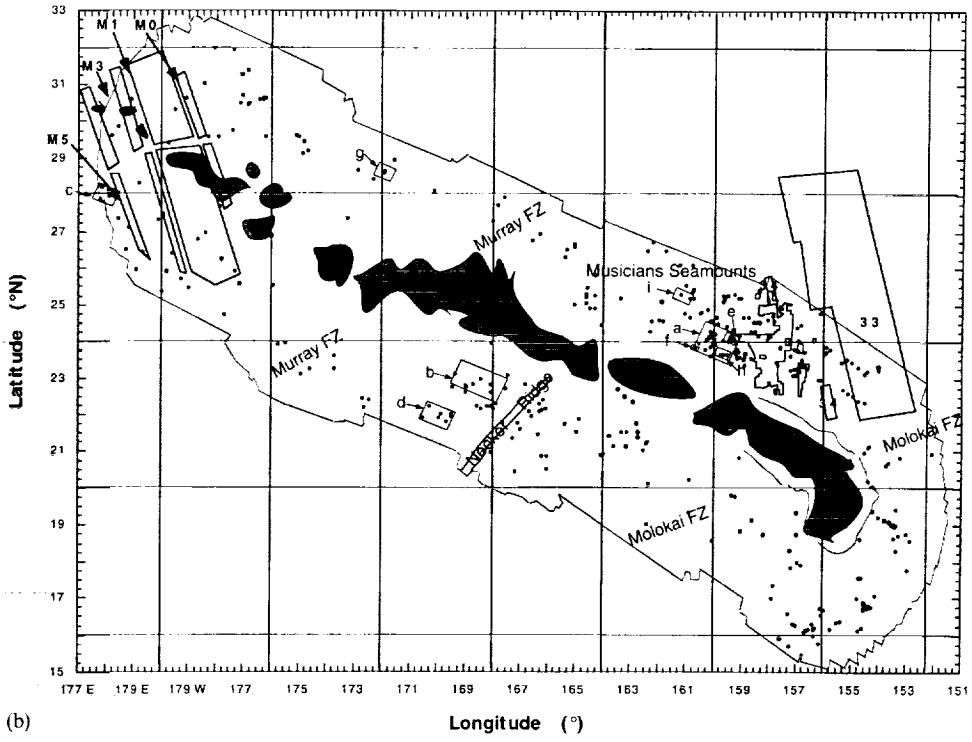
M1
M0
M3
M5
Murray FZ
Musicians Seamounts
Murray FZ
Necker Ridge
Molokai FZ
Molokai FZ
Latitude (°N)
Longitude (°)
177 E 179 E 179 W 177 175 173 171 169 167 165 163 161 159 157 155 153 151
33 31 29 27 25 23 21 19 17 15

(b)

caused lithospheric flexure, producing a discontinuous moat known as the Hawaiian Deep ranging in depth from ~4000 to ~5600 m (Fornari and Campbell, 1987; Moore, 1987; Moore et al., 1989). The Deep is filled with debris shed from the islands in the form of slump blocks and giant landslides, some of which lap onto the Deep's outer edges (Moore et al., 1989, 1994). Outside of this depression is the Hawaiian Arch, a low (200 m) and broad upbowing of the seafloor resulting from flexural compensation of the displaced material of the Deep (Wessel, 1993; Wessel and Keating, 1993; Moore et al., 1994). The North Arch, between the Murray and Molokai FZ's, contains a large Pliocene–Pleistocene alkalic lava flow field that is clearly visible in sonar imagery (Fig. 2a; Clague et al., 1990).

Seaward of the Deep are hundreds of seamounts, most of which have not been sampled or described. Some of these, such as Loihi southeast of the Big Island, result from volcanism associated with the Hawaiian hotspot. North of the main islands, another hotspot on young (<15 Ma) crust near the ancestral EPR may have formed some of the Musicians seamounts (Pringle, 1993). In the present day, the most prolific site for seamount genesis in the Pacific is adjacent to the axis of the EPR (Smith and Jordan, 1988; Smith, 1991; Scheirer and Macdonald, 1995). Thus, it is reasonable to assume that many, if not most, of the seamounts seen near Hawaii also formed near the EPR and are thus nearly the same age as the underlying crust.

Due to the scarcity of samples and in situ reconnaissance studies of these and other seamounts, studies rely heavily on sonar and other remote sensing methods. This paper discusses the seamounts near Hawaii as viewed by the *GLORIA* sonar. The primary purposes of this work are: (1) to document the characteristics, distribution, and associations of the seamounts; (2) to compare the seamounts to others elsewhere in the Pacific; and (3) discuss what the sonar data allows us to infer about the seamounts' origin.

2. Data and methods

The region examined in this study, the U.S. Hawaii Exclusive Economic Zone (HEEZ) has an area of 2.38×10^6 km^2 and an irregular boundary bounded by 15–33°N and 151°W–178°E (Fig. 1). Mapping of the HEEZ with the *Geologic LOng Range Inclined ASDIC* (*GLORIA*) digital side-scan sonar system took place during 1986–1991. The source and receiver of the sonar were located in a "fish" towed ~200 m behind the ship (Gardner, 1992). Sonar pulses were emitted about every 30 s. The seafloor was imaged on either side of the ship track out to an average horizontal distance of ~12.5 km at a spatial resolution of ~50 m. The energy or amplitude of the returned signals was stored as digital data. These were then combined into images depicting backscatter intensity as shades of gray, with white corresponding to the highest energy. High backscatter results from surfaces that are rough at the scale of the *GLORIA* sonar wavelength (22–24 cm, or 6.3 and 6.7 kHz; Geyer, 1992), such as lava, or from slopes oriented perpendicular to the beam path. In addition to the backscatter sonar information, depth at nadir was recorded with a wide-beam echo sounder at a vertical resolution of ~1 m (W. Normark, pers. commun., 1994).

Fig. 1. Maps of the distribution of seamounts found in the *GLORIA* mosaic of the Hawaiian Exclusive Economic Zone (see text for identification criteria). *Light, straight lines* define the boundary of the map area. *Dark shaded region* is the approximate area of the Hawaiian Ridge. Area labeled *Musicians Seamounts* is southern part of area containing large seamounts of this name. *Labels* for fracture zones and the Necker Ridge are along approximate trends and locations. *Numbered boxes* are normal magnetic anomalies (from map of Atwater and Severinghaus, 1988): anomaly 33≈75–80.5 Ma, 34≈<84.5 Ma, M_0≈118 Ma, M_1≈122 Ma, M_3≈123.5–125.5 Ma, M_5≈127 Ma).

a. Distribution map as a function of seamount diameter.

b. Distribution map showing prominent seafloor features. The Hawaiian Deep is shown in *light outline* around the east end of the ridge. *Rectilinear outline* to north of eastern ridge is the approximate boundary of the North Arch lava flow field. Delineation of the Necker Ridge is shown as a *dark outline*. *Lettered boxes* are the boundaries of the images in Fig. 2.

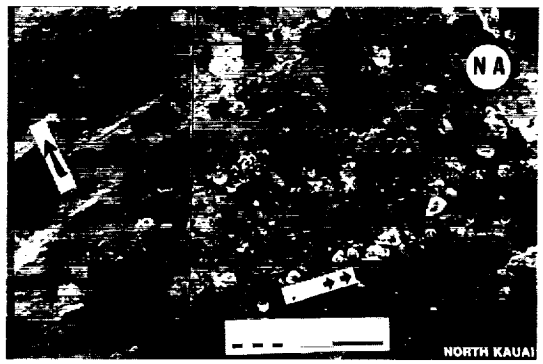

(a)

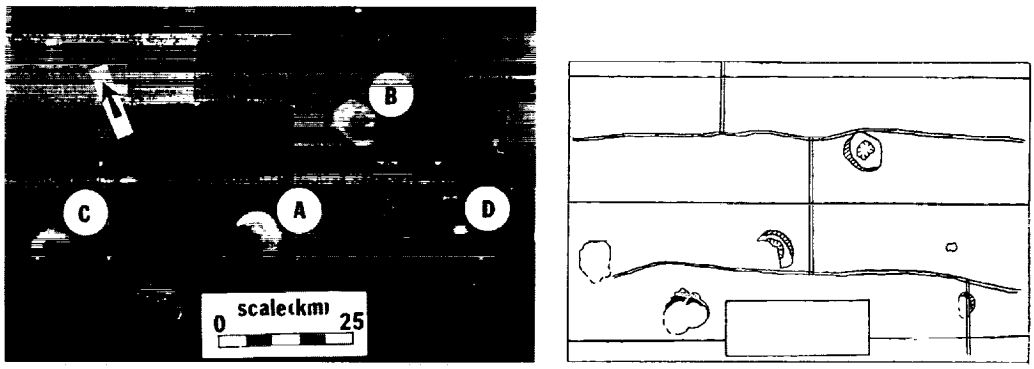

(b)

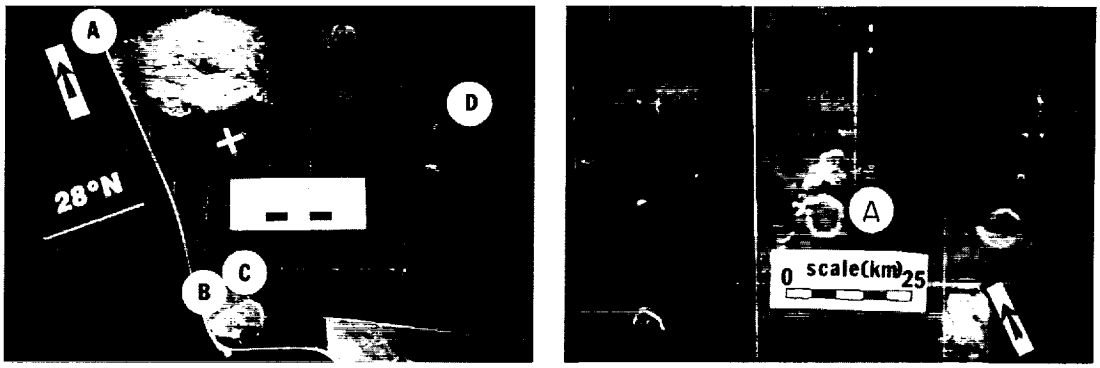

(c) (d)

Fig. 2. *GLORIA* images of seamounts in the HEEZ. Brightness is proportional to sonic backscatter. Prominent *horizontal lines* delineate ship tracks. *Black arrow* in all pictures indicates north. *Coordinates* at the end of each caption are the approximate latitudes and longitudes at the center of the image. Outlines of the images are shown in Fig. 1b.

a. Field near the Musicians seamounts. Note the alignment of some of the constructs, direction of which are shown by *arrows*. The western portion of the North Arch lava flow field (*NA*) is seen as a sonar-bright region on the right-hand side of the image (24°N, 160°W).

b. *Left*: Image of seamount field. Seamount with a truncated edge is indicated by *A*. It appears to have a crater in its center, as does the large volcano in the upper right (*B*). Far left volcano is representative of a heap (*C*), and the small, bright volcano at center-right is a typical cone (*D*) (23°N, 169°W). *Right*: Sketch of seamount field. *Horizontal* and *vertical double lines* are boundaries between mosaic pieces. *Horizontal single lines* are ship tracks. Seamount boundaries and features delineated as *solid* where certain, *dashed* where uncertain. *Hatchures* = crater; *diagonal line fill* = sonar-bright edge; *dark fill* = sonar shadow; *stipples* = landslide deposit.

c. A large irregular heap seamount (upper left, *A*) and two coalesced pancake volcanoes (lower left, B and C) (28°N, 178°E). *D* is the seamount shown in profile in Fig. 7.

d. A seamount fairly representative of the pancake class (*A*). It is illuminated on both sides because mosaic frames are joined through its center (22°N, 170°W).

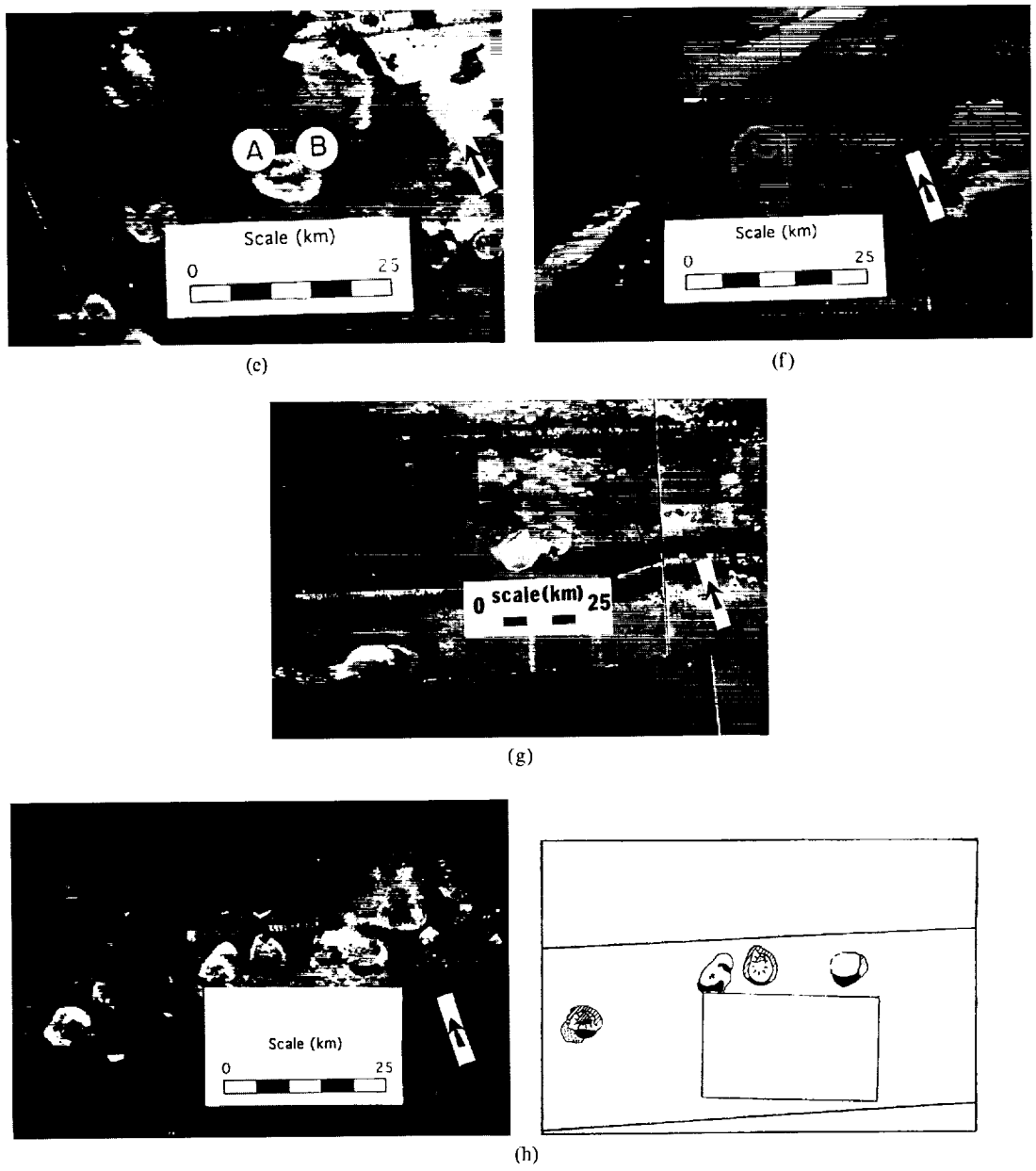

Fig. 2.e. Seamount with two large craters (*A* and *B*). Bright terrain in upper right is a portion of the North Arch lava flow field (24°N, 159.5°W).

f. Elongated seamount with a large crater (24°N, 161°W).

g. Coalesced seamounts. Note mound atop the right volcano, indicated by an *arrow* (28.5°N, 172°W).

h. *Left*: Image of seamount field. Mounds on seamount summits are shown by *arrows*. Bright material on SW flank of seamount labeled *L* may be a landslide deposit (23.6°N, 159.8°W). *Right*: Sketch of seamount field. *Nearly horizontal lines* cutting across image are ship tracks. Seamount boundaries and features delineated as *solid* where certain, *dashed* where uncertain. *Hatchures* = mound; *diagonal line fill* = sonar-bright edge; *dark fill* = sonar shadow; *stipples* = landslide deposit.

(i)

Fig. 2.i. Seamount disrupted by a graben (25.3°N, 161.2°W).

In this study, the *GLORIA* sonar image mosaic of the Hawaii EEZ was used to identify and visually inspect seamounts distal from the Hawaiian Ridge. The mosaic consists of individual side-scan sonar imagery strips pasted together parallel to the ship tracks (Fig. 2b) and provides a synoptic view of the HEEZ. The distinguishing characteristics used to identify volcanic constructs as "seamounts" were a circular to semi-circular outline and a sonar-brightness different than the surrounding seafloor. This term is not restricted to a specific size range or mode of origin.

To subdivide the seamount population, a qualitative classification was applied to each volcano. Constructs with a generally equant shape and a fairly uniform, bright appearance on the sonar-facing side were classified as "cones" (Fig. 2b). These were interpreted as more or less conical structures lacking wide, flat tops. At the other end of the scale, seamounts with a homogeneous sonar-gray interior commonly surrounded by a well-defined bright annulus on the sonar-facing edge were interpreted as flat-topped, steep-sided "pancake" constructs (Fig. 2c and d). The remaining volcanoes commonly were more amorphous and generally lacked a distinct contrast between their edge and interior. They were interpreted as irregular masses of lava and sediment and classified as "heaps" (Fig. 2b). In a few cases amorphous heaps were found to form elongated ridges and were designated "ridge mounds". Rare, generally large seamounts with prominent radiating, sonar-bright spines probably representing flank rift zones (Vogt and Smoot, 1984) were classified as "stars". The classification is not perfect. For one, sonar brightness is a function not only of topography, but also of the cm-scale roughness of the surface and near-surface materials (Barone and Ryan, 1990). In some cases it was difficult to determine whether brightness variations were caused only by topography or were also influenced by the distribution of sonar-bright lava and sonar-dark sediment. Indeed, as will be discussed in greater detail later, the limited bathymetry available for pancake seamounts shows that they are not as steep-sided or flat-topped as they appear to be in sidescan imagery. Second, regardless of the brightness problem, simply classifying the seamounts was often difficult and somewhat subjective. The seamounts have a range of morphologies that do not necessarily represent distinct end-members. The reader is urged to consult other seamount studies that employ side-scan sonar for further discussion of these and other problems (e.g., Searle, 1983; Fornari et al., 1987a; Barone and Ryan, 1990; Scheirer and Macdonald, 1995).

The approximate positions of the seamounts were found from fiducial marks on the mosaic edges and by comparison to an unpublished accompanying map (prepared by R. Holcomb). Maximum and minimum diameter were compiled for each seamount. Special geomorphological features associated with the seamounts, such as the presence of summit craters, landslides, and erosional features, also were compiled. These data are listed in Appendix A.

An attempt was made to measure seamount heights from the bathymetric maps of Chase et al. (1992). However, because the maps were produced by interpolation of scattered bathymetric measurements, they generally lacked the spatial resolution to identify most seamounts. In addition, no maps were available for the western half of the HEEZ at the time of this study. HEEZ data from *Seabeam*, a wide-beam echo sounder superior to *GLORIA* in characterizing seamount shapes, cover few of the regions where seamounts are found in this study. Thus, except for two *GLORIA* bathymetry measurements discussed later, height was not investigated.

3. Observations and results

3.1. Quantitative characteristics

Over the area of the Hawaii EEZ, 390 seamounts greater than 1 km in diameter were found (Figs. 1 and 2; Appendix A). This gives an areal density of 164 seamounts per 10^6 km^2 for this size range. Factoring out the ~10% of the region occupied by the Hawaiian Ridge, the abundance is 182 volcanoes/10^6 km^2.

The diameters of the HEEZ seamounts range from ~1 to 57 km. Only 18 seamounts (5%) are larger than 15 km. Plotting relative abundance vs. diameter of seamounts ≤16 km in diameter in 2-km bins shows that the modal diameter group is between 2 and 4 km (Fig. 3). The number of seamounts increases fairly steadily down to diameters of 2 km, after which there is a large drop. This decrease is probably due to the difficulty in identifying small seamounts with the available data.

In order to compare the size distribution of the HEEZ seamounts to other Pacific data sets, the cumulative seamount abundance as a function of diameter was plotted in Fig. 4 and fit to the exponential equation:

$$v(D) = v_0 \exp(-\alpha D) \quad (1)$$

where $v(D)$ is the cumulative abundance of seamounts of diameter $d \geq D$ per unit area; v_0 the total number of seamounts of all sizes greater than zero per unit area; and α^{-1} the characteristic diameter (Jordan et al., 1983; Smith and Jordan, 1988). α determines the slope of the abundance–diameter exponential line fit, with greater characteristic diameters giving shallower slopes. α and v_0 were computed using the methods of Jordan et al.

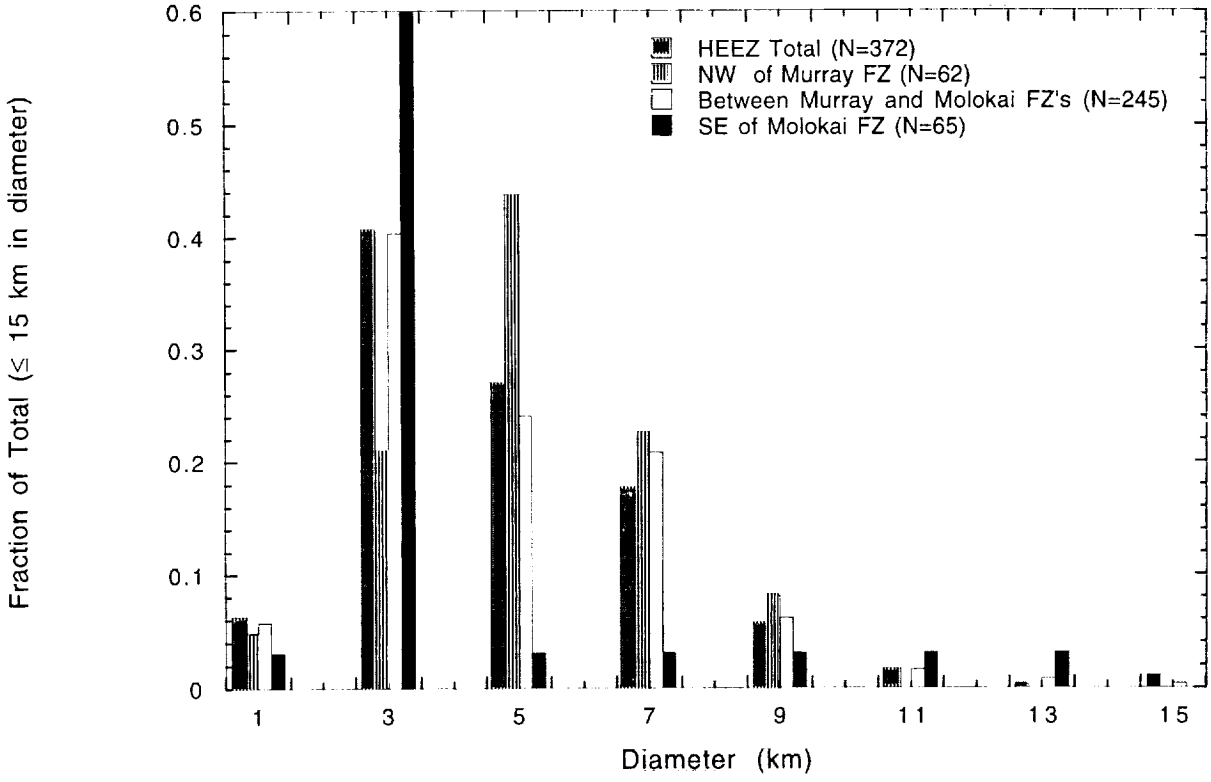

Fig. 3. Diameter vs. fractional abundance, normalized to the number of seamounts in each of the four regions. The bins are 2 km wide, centered on the value listed, inclusive at their lower boundary and exclusive at their upper. Seamounts with diameters greater than 16 km are not included.

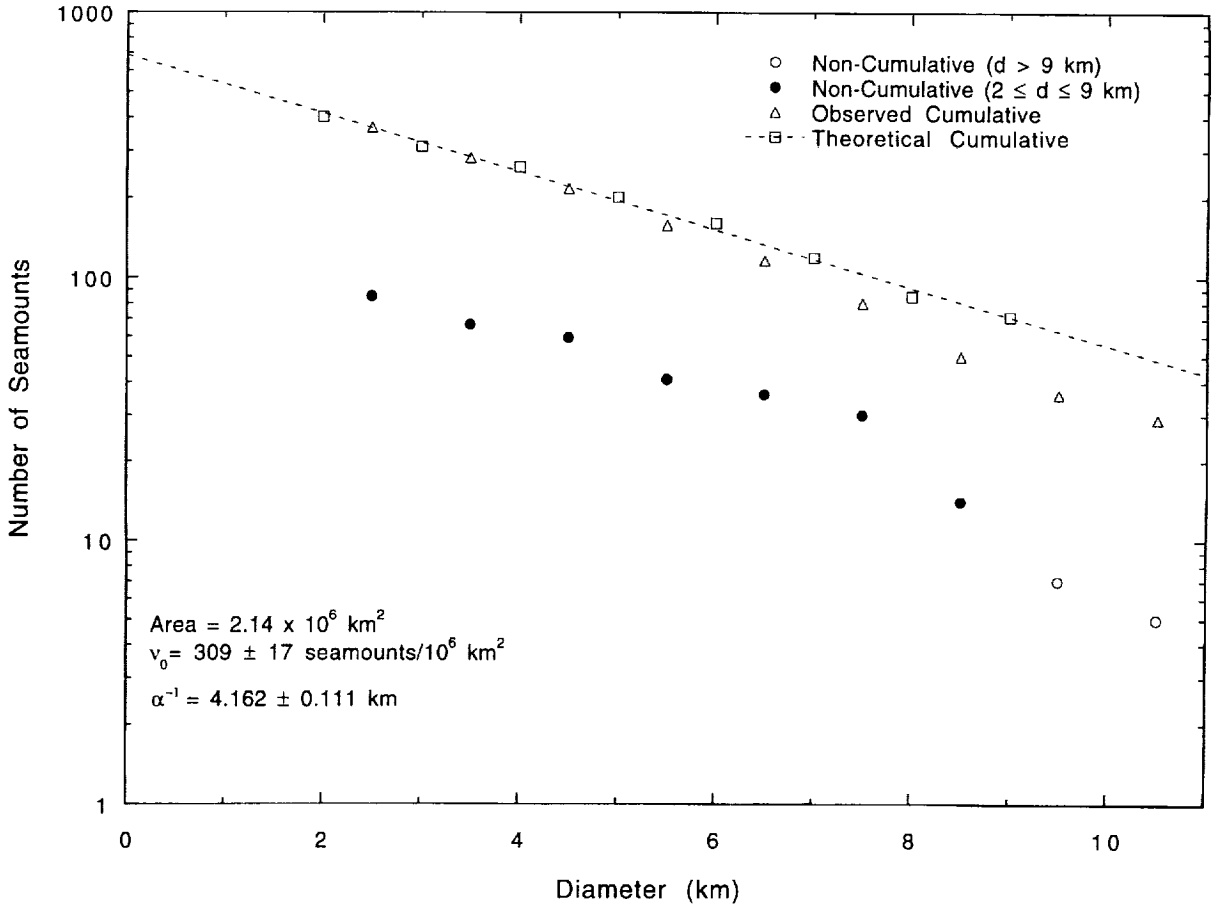

Fig. 4. Abundance and cumulative abundance vs. diameter in 1-km bins for the whole HEEZ. Non-cumulative diameter bins are 1 km wide, centered on the value listed, inclusive at their lower boundary and exclusive at their upper. *Open circles* were eliminated in the statistical analysis to compute v_0 and α^{-1}. The theoretical cumulative counts are not actual values, but assume a statistically derived number of seamounts larger than the maximum size found, as explained in Smith and Jordan (1988).

(1983) and Smith and Jordan (1988). α^{-1} and v_0 for the whole HEEZ, minus the area of the Hawaiian Ridge, are 4.16 ± 0.11 km and 309 ± 17 seamounts/10^6 km^2, respectively (Fig. 4).

3.2. Morphology

The distribution of the seamounts as a function of morphologic class is shown in Fig. 5. Out of the volcano population, 127 (33%) were classified as heaps (Fig. 2c), 38 (10%) were categorized as cones (Fig. 2b), 6 (2%) were labeled stars, and 3 (1%) were called ridge mounds. The remaining 216 (55%) were classified as pancakes (Fig. 2c and d).

The seamounts are generally bilaterally symmetric. They commonly exhibit distinct morphologic features and the compilation reveals the most prevalent forms (Fig. 6). Sixty-two volcanoes, or 16% of the data set, have one or more central craters (Figs. 2e–f). Forty-three (11%) are surmounted by one or more mounds (Fig. 2g and h). Seventeen (4%) consist of an apparent grouping of coalesced volcanoes that together make up a larger structure (Figs. 2b and g). Nine (2%) have edges that are truncated (Fig. 2b). Nine (2%) have landslides on their flanks (Fig. 2h). Three (1%) are cut by graben (Fig. 2i), with strikes of ENE–WSW (the one pictured in Fig. 2i), NE–SW,

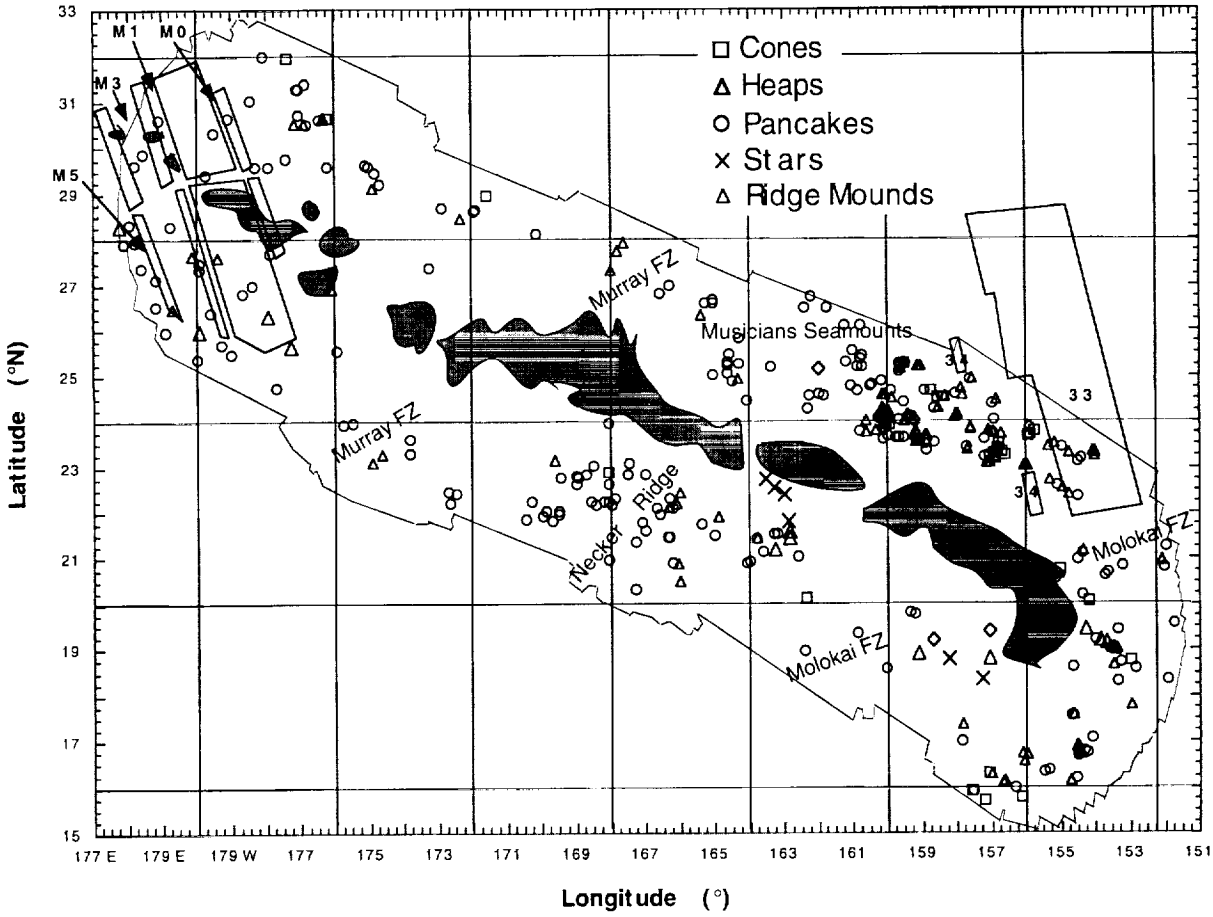

Fig. 5. Same as Fig. 1, but showing seamounts by class.

and NW–SE. The remaining volcanoes (260; 67%) lack these special features.

To gain some insight into the cross-sectional shapes of the HEEZ seamounts, wide-beam echo-sounding measurements were retrieved from raw bathymetric records. Depth measurements were restricted to lines directly below the ship, so that only two profiles crossing seamounts were obtained. One profile, at 27.4° N, 178.4°E, is shown in Fig. 7. The seamount as seen on the *GLORIA* mosaic is shown in Fig. 2c. Maximum height above the seafloor along the cross-section is 42 m and the width is 4.4 km. This gives a cross-section aspect ratio (height/diameter) of 0.01. In contrast, most Pacific seamounts have aspect ratios near 0.1, although some are as low as 0.03 (Smith, 1988). This profile may be through the center of an anomalously low aspect ratio seamount. More likely, the seamount probably has an aspect ratio somewhat larger than 0.01, but the profile is on the flank of the structure. Another profile, near 21.5°N, 163.2°W (Fig. 8) has a maximum height beneath the track of 305 m. It is 8.9 km wide along track, giving a cross-section aspect ratio of 0.03. Its steepest slopes, enhanced in appearance by the vertical exaggeration, are at the base. Although both of these seamounts look like pancakes in the *GLORIA* mosaic, one is clearly much flatter than the other. This is a reflection of the difficulty of visually distinguishing the morphology of anything

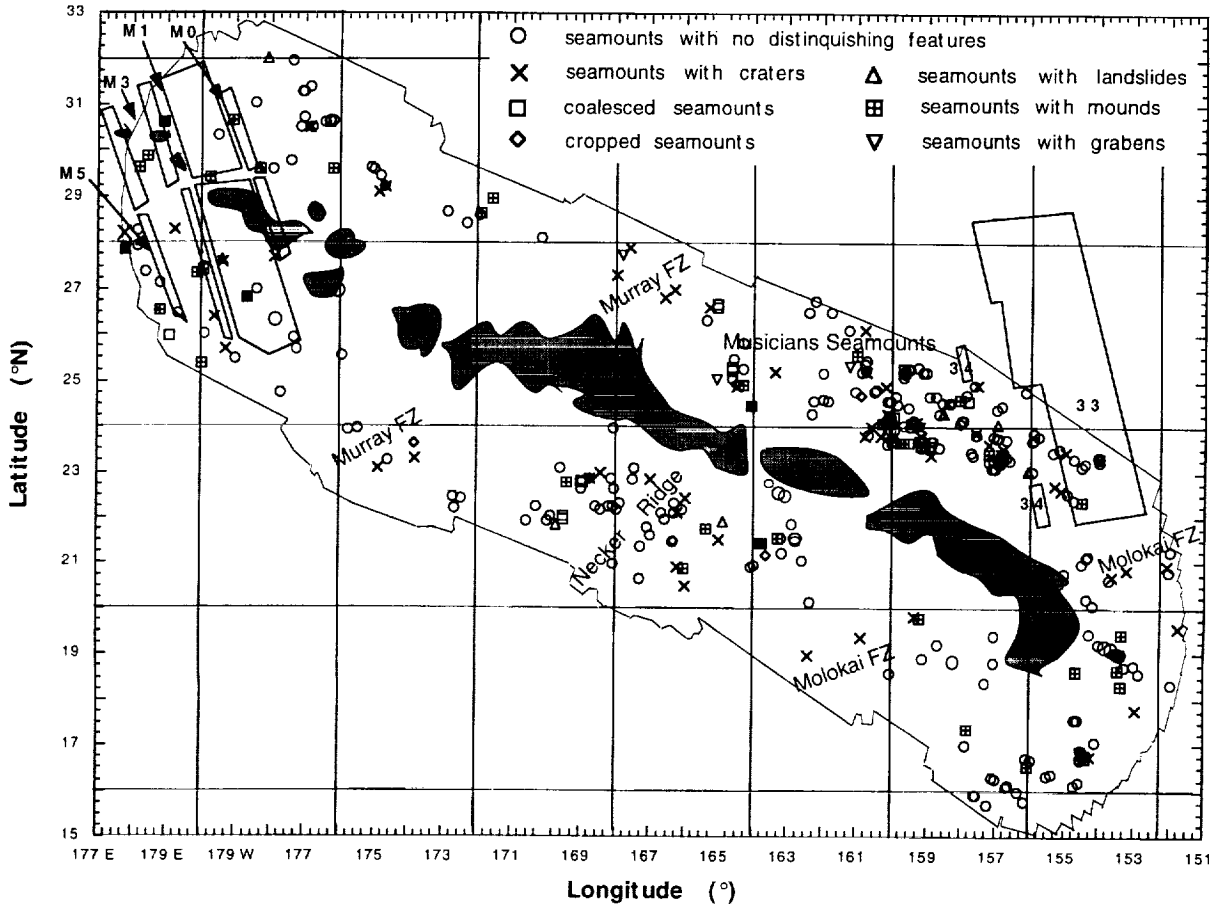

Fig. 6. Same as Fig. 1, but showing seamounts by type of ancillary feature. *Symbols* are superimposed where more than one ancillary feature is present.

near nadir. The problems with nadir viewing also make it difficult to assess the position of the bathymetric track atop the seamount.

3.3. Regional variations

Regional variations were examined to see if location or tectonic setting affected the areal density, size distribution, and characteristics of the HEEZ seamounts. In general, seamount distribution is clumpy, with only a few isolated volcanoes (Fig. 1). In some cases, the seamounts are densely clustered and two or more are merged, forming a single "coalesced" edifice (see above). The seamounts are concentrated mostly north of the islands. Within this region, some seamounts are aligned along the same trend as the fracture zones (Fig. 2a). In the south-central region, many seamounts are aligned along a trend parallel to the Necker Ridge (Fig. 1). Fewer seamounts are located in the west-central and southeast-central regions of the map area. Within 1° × 1° quadrangles away from the Hawaiian Arch, the minimum number of seamounts is zero, and the maximum number is 18 (24–25°N, 160–161°W, within the southern Musicians seamounts and between the Murray and Molokai FZ's). No geographic clustering of volcanoes by class (Fig. 5) or distinguishing feature (Fig. 6) is apparent.

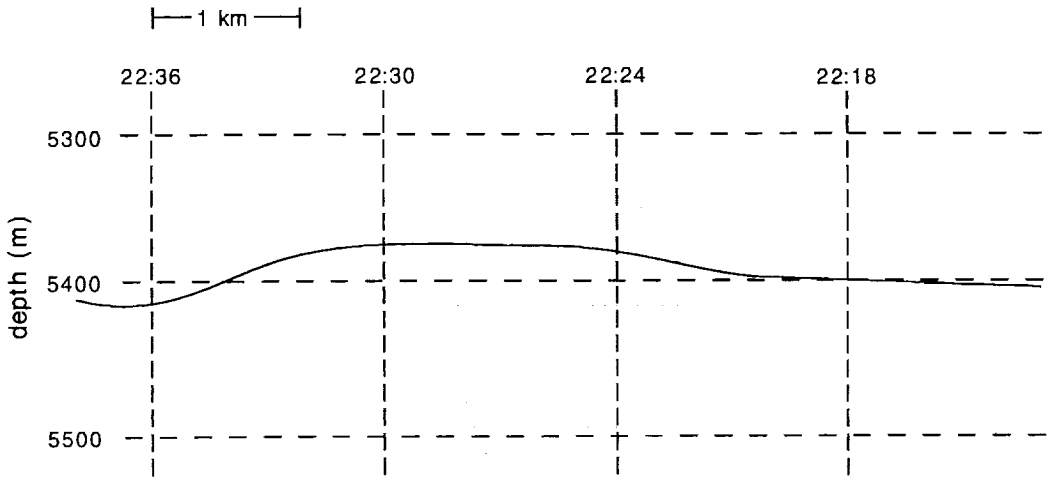

Fig. 7. Profile of a seamount at 27.4°N, 178.4°E from the nadir-viewing wide-beam *GLORIA* echosounder. Depth in meters is shown on the left side. The *top numbers* are the time at which the ship was over this part of the seafloor. With a ship speed of 8 knots (W. Normark, pers. commun., 1994), each 6-min block on the diagram is equivalent to ~1.5 km. The vertical exaggeration is slightly greater than 9×. This seamount is labeled *D* in Fig. 2c.

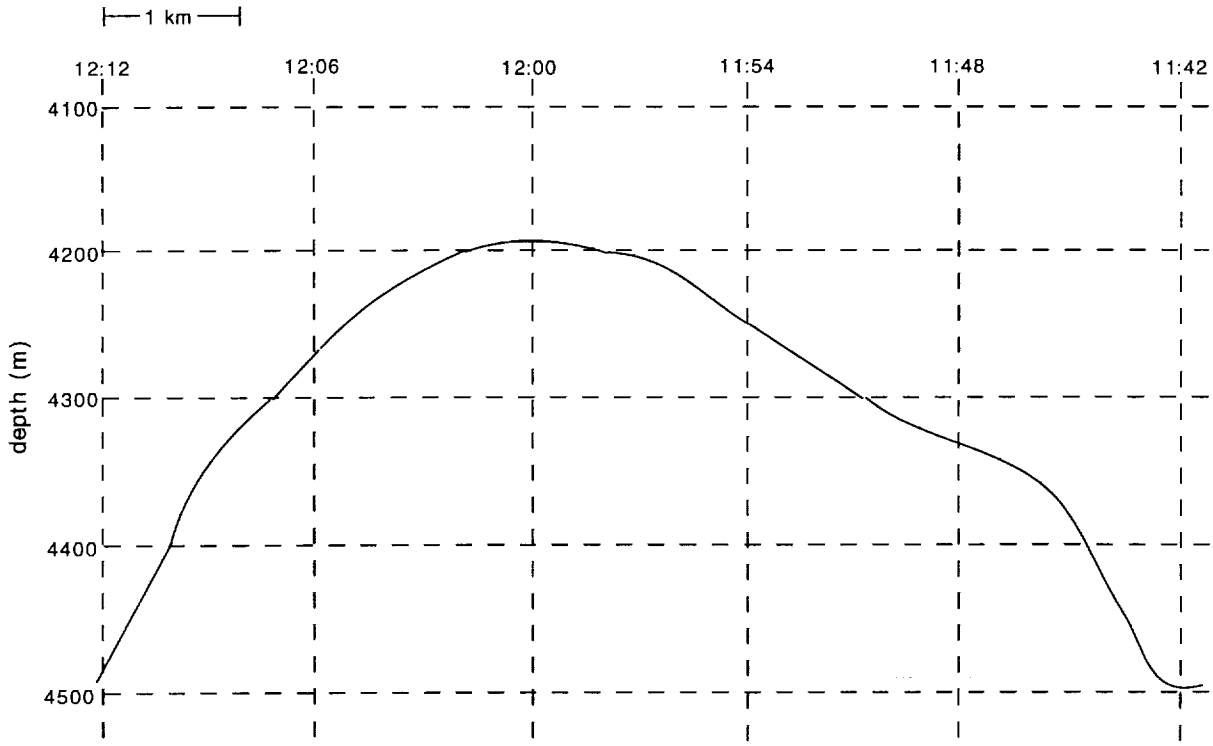

Fig. 8. Profile of a submarine volcano at 21.5°N, 163.2°W. *Axes* same as in Fig. 7. The vertical exaggeration is slightly greater than 10×.

The Murray and Molokai FZ's trend roughly perpendicular to the strike of the Hawaiian Ridge and divide the HEEZ into three tectonic regions. In the area northwest of the Murray FZ, which includes ~40% of the HEEZ, 67 seamounts larger than 1 km were found, for a density of 78 seamounts/10^6 km^2 (area excludes the Hawaiian Ridge). The theoretical areal density of seamounts of all sizes (v_0) and characteristic diameter (α^{-1}) are $(212\pm28)/10^6$ km^2 and 17.7 ± 0.4 km, respectively (Table 1). The 40% of the HEEZ between the Murray and Molokai FZ's has 250 seamounts larger than 1 km ($292/10^6$ km^2). v_0 and α^{-1} are 503 ± 34 seamounts/10^6 km^2 and 4.48 ± 0.13 km, respectively (Table 1). This region contains the Pliocene–Pleistocene North Arch lava flows and associated vents (Clague et al., 1990). The remaining 20% of the HEEZ southeast of the Molokai FZ has 73 observed seamounts larger than 1 km ($171/10^6$ km^2). v_0 is 187 ± 26 seamounts/ 10^6 km^2 and α^{-1} is 4.88 ± 0.32 km (Table 1). A correlation of magnetic anomalies adjacent to the Cretaceous quiet zone (Atwater and Severinghaus, 1988) indicates that the seafloor between the Murray and Molokai FZ's is ~17 Myr younger than the adjacent tectonic regions, so that the youngest crust in this region of the Pacific has the most seamounts.

The seamounts SE of the Molokai FZ and between the two fracture zones have modal diameters of 2–4 km like that found in the overall HEEZ (Fig. 3). Northwest of Murray the modal diameter is larger, at 4–6 km. The seamounts southeast of the Molokai FZ in the 2–4-km bin represent 60% of the population of this region, the largest fraction occupied by any 2-km bin for the three tectonic regions and the overall HEEZ.

No prominent trends of seamount diameter parallel to the strike of the Hawaiian Ridge are apparent (Fig. 9a). Seamount morphologic classes show no trends or clumping in this direction nor do they favor any particular tectonic zone. Plotting diameter vs. distance perpendicular to the strike of the Murray and Molokai FZ's shows that seamounts near the fracture zones have, on average, smaller diameters and are fewer in number than more distal ones (Fig. 9b and c, respectively). The distribution of morphologic classes relative to the fracture zones is random. Note that the irregular boundary of the map area somewhat inhibits a completely rigorous statistical analysis of seamount distribution.

Table 1
Pacific seamount areal density (v_0) and characteristic diameter (α^{-1})

Region	v_0	v_2	v_6	α^{-1} (km)	Source
HEEZ	309 ± 17 (182)	191 ± 11 (171)	73 ± 4 (54)	4.16 ± 0.11	this study
NW of Murray fracture zone in HEEZ	212 ± 28 (78)	189 ± 25 (75)	151 ± 20 (28)	17.68 ± 0.36	this study
Between Molokai and Murray fracture zones in HEEZ	503 ± 34 (292)	322 ± 22 (276)	132 ± 9 (91)	4.48 ± 0.13	this study
SE of Molokai fracture zone in HEEZ	187 ± 26 (171)	124 ± 17 (156)	55 ± 8 (33)	4.88 ± 0.32	this study
Pacific (average of 8 areas)	5440 ± 650			3.17 ± 0.4	Jordan et al. (1983); Smith and Jordan (1988)
Between Clarion and Murray fracture zones, East Pacific ("Area 1")	6750 ± 2050			2.57 ± 0.38	Smith and Jordan (1988)
Between Murray and Mendocino fracture zones, East Pacific ("Area 2")	1660 ± 650			3.08 ± 0.67	Smith and Jordan (1988)

Values of v for an area of 10^6 km^2; subscript of v is the seamount diameter (km) equal to and above which theoretical cumulative seamount abundances were computed; values in parentheses are actual abundances per 10^6 km^2. α^{-1} for areas "1" and "2" converted from characteristic height by assuming a seamount height to diameter (aspect) ratio of 0.1.

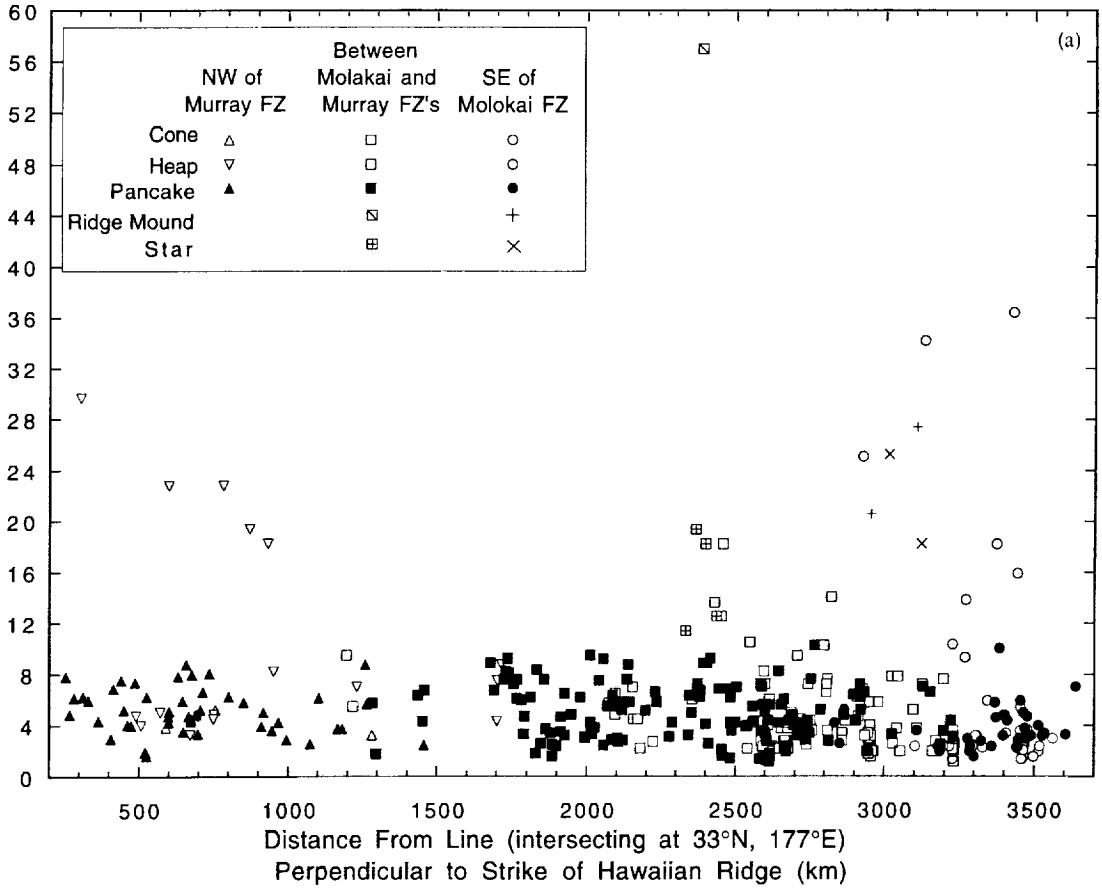
(a)
NW of Murray FZ
Between Molakai and Murray FZ's
SE of Molokai FZ
Cone
Heap
Pancake
Ridge Mound
Star
Distance From Line (intersecting at 33°N, 177°E)
Perpendicular to Strike of Hawaiian Ridge (km)

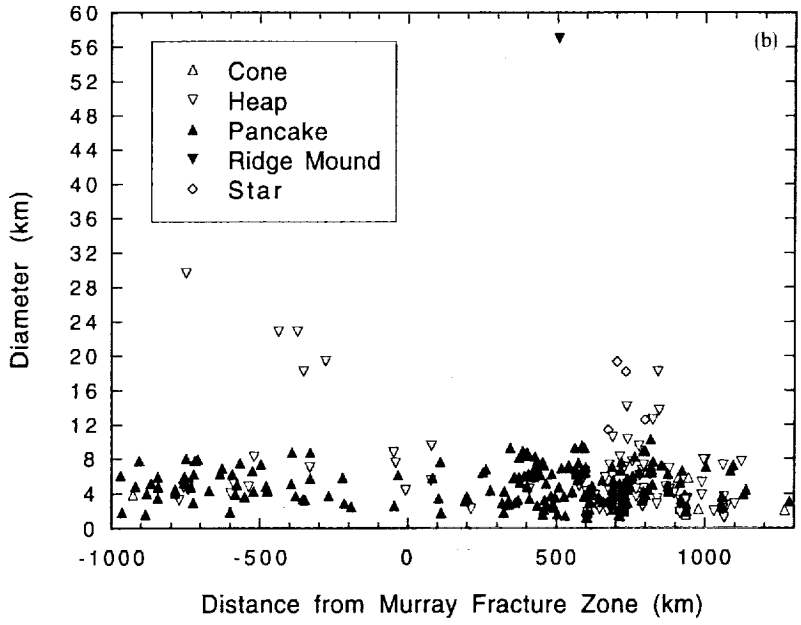
(b)
Cone
Heap
Pancake
Ridge Mound
Star
Diameter (km)
Distance from Murray Fracture Zone (km)

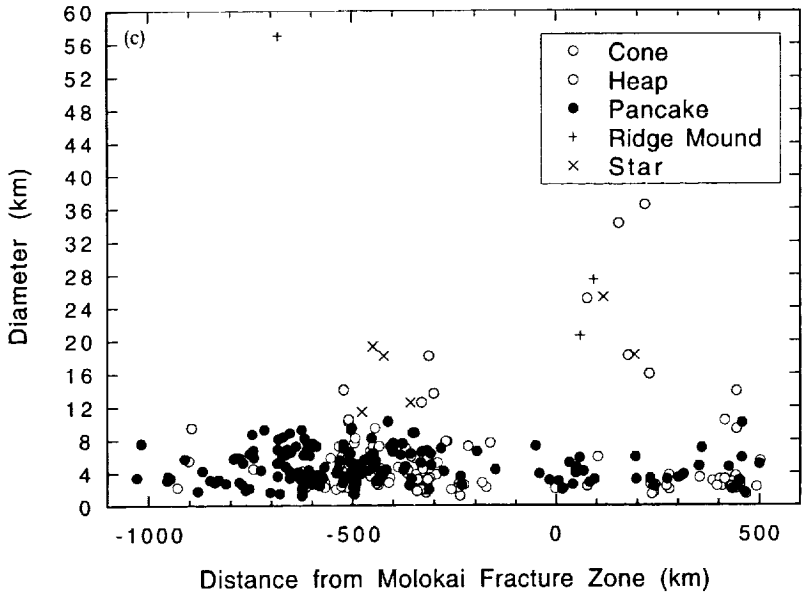

Fig. 9. a. Seamount diameter vs. distance (km) from a line perpendicular to the strike of the Hawaiian Ridge that intersects 33°N, 177°E (near the northwest extent of the HEEZ).

b. Seamount diameter vs. distance (km) from the strike of the Murray Fracture Zone. Negative values are west of the fracture zone, positive values are east. The eastern end of the plot is near the Molokai Fracture Zone.

c. Seamount diameter vs. distance (km) from the strike of the Molokai Fracture Zone. Negative values are west of the fracture zone, positive values are east. The western end of the plot is near the Murray Fracture Zone.

4. Comparisons to other Pacific seamounts

4.1. Abundances and distributions

The theoretical concentration of seamounts from the exponential model (v_0) of 309 ± 17 per 10^6 km^2 in the HEEZ is much less than that determined in most other Pacific regions using modern high-resolution sonar surveys (Table 2) (Smith, 1991). Smith and Jordan (1988), in their study of seamount statistics in eight areas of the Pacific, estimated an average v_0 of 5440 ± 650 seamounts/10^6 km^2. This was based on 11,506 km of *Seabeam* tracks in the eastern Pacific in which 186 seamounts having heights from 100 to 1100 m were found. None of the areas in their study included the HEEZ. The two closest regions are their areas 1 and 2. Area 1 is between the Clarion and Murray FZ's and extends from the eastern HEEZ boundary to near the southern Californian and northern Mexican coasts. Area 2 is between the Murray and Mendocino FZ's and extends from north of the HEEZ to near the northern Californian coast. The theoretical areal densities in areas 1 and 2 are 6750 ± 2050 and 1660 ± 650 seamounts/10^6 km^2, respectively. The lesser theoretical abundance of seamounts in area 2 relative to area 1 (i.e., north and south of the Murray FZ, respectively) is consistent with the theoretical areal density contrasts found here (212 ± 28 vs. 503 ± 34) (Table 1). Thus, although the absolute abundances of seamounts differ between this study and that of Smith and Jordan, the decrease in predicted abundances going north across the Murray FZ agree.

The alignment of some HEEZ seamounts along the trends of fracture zones is analogous to seamount chains aligned parallel to the spreading direction and transform faults adjacent to the modern EPR (Batiza and Vanko, 1983; Fornari et al., 1984; Macdonald et al., 1984; Lonsdale, 1985; Macdonald, 1989; Scheirer and Macdonald, 1995). It is therefore likely that these seamounts are about the same age as the underlying crust. For EPR-derived seamounts, the abundance con-

Table 2
Pacific seamount areal densities per 10^6 km^2 (modified from Smith, 1991)

Region	Data	All sizes	h					Reference
			≥ 50 m	≥ 100 m	≥ 300 m	≥ 500 m	≥ 1000 m	
Actual counts:								
Pacific wide-beam profiles							62	Menard (1959)
Baja CA smt. prov.	wide-beam profiles						714	Menard (1959)
SE Pacific	maps, wide-beam profiles					40	15	Cailleux (1975)
Pacific maps						40		Udistsev et al. (1976)
N Pacific (≤136 Ma)	maps				124			Batiza (1982)
S Pacific (≤136 Ma)	maps				57			Batiza (1982)
Nazca Plate	*GLORIA* side-scan			1410				Searle (1983)
Hawaii EEZ	*GLORIA* side-scan			182[a]				this study
Theoretical estimates:								
E Pacific (≤65 Ma)	wide-beam profiles				1633 ± 416	905 ± 228	207 ± 62	Jordan et al. (1983)
EPR 0–24°N (≤10 Ma)	multibeam swaths		9000					Fornari et al. (1987b)
S. Pacific (≤40 Ma)	multibeam swaths		9645 ± 449			55 ± 14		Abers et al. (1988)
Pacific (8 areas)	wide-beam profiles	5440 ± 650			1920 ± 116	959 ± 30	169 ± 17	Smith and Jordan (1988)
Hawaii EEZ	*GLORIA* side-scan	309 ± 17						this study

[a]Found by assuming that the HEEZ seamounts have an aspect ratio of 0.1.

trasts across the fracture zones can be explained in two ways (Bemis and Smith, 1993): (1) at the EPR, more seamounts were produced on one side of a fracture zone than on the other side; and (2) volcanic production was episodic through time at the EPR, resulting in different seamount abundances on crust of different age.

Localized igneous activity since leaving the EPR could also contribute to the greater abundance of seamounts between the Murray and Molokai FZ's. Some of the Musicians seamounts in this region are up to 15 Myr younger than the crust upon which they rest and may result from an old hotspot that resided off-axis from the ancestral EPR (Pringle, 1993). The Pliocene–Pleistocene North Arch lava flows show that even more recent igneous activity has occurred in this region. The lithosphere in this region is younger and thinner than that on the other side of the fracture zones and may allow more decompression melting from a hotspot source (Phipps Morgan et al., 1995). Finally, the *GLORIA* images show that some seamounts in the region are aligned next to and along the same trend as the Necker Ridge, suggesting a contemporaneous age that is younger than the underlying crust. Thus, in addition to the dated Musicians, other seamounts may be young. However, unequivocal resolution of the question of whether or not great abundances of young seamounts exist must await future sample collection and analysis.

Two factors may account for the *overall* low relative abundance of HEEZ seamounts. The first is sediment cover. Sediment thickness is, on average, less in areas 1 and 2 of Smith and Jordan (1988) than in the HEEZ (Winterer, 1989). There are no strong variations in biological productivity between these regions, so that the main reason for the contrast in thickness is the younger crust in areas 1 and 2. Assuming a sediment deposition rate of 2.5 m/Myr (Moore et al., 1994) and an age of HEEZ crust between 72 Ma (magnetic anomaly 33) and 130 Ma (anomaly M10) (Atwater and Severinghaus, 1988), sediment cover on EPR-derived HEEZ seamounts should range from 180 to 325 m. This estimate is consistent with 235 m of sediment found in cores from Ocean Drilling Program Sites 842 and 843 south of the Hawaiian Arch at 19°N, 159°W (Hull, 1993). Assuming the HEEZ seamounts have aspect ratios of 0.1, 250 m of sediment should decrease their diameters by 2.5 km and bury them completely if they are smaller. The low backscatter of sediment relative to basalt should make buried seamounts difficult to see in *GLORIA* imagery, even if some topographic signature is preserved. If this sediment is "removed" by increasing the diameter of the seamounts by 2.5 km, v_0 nearly doubles to 576 ± 58 seamounts/10^6 km^2. This value is still far lower than the values of Smith and Jordan (1988). Furthermore, the estimate is too liberal if some of the seamounts formed since leaving the EPR, because they should have less sediment cover.

The different methods used to identify seamounts are probably a significant additional factor. Smith and Jordan (1988) used bathymetric tracks, not visual imagery, for identification. In the earlier studies, misidentification of volcanoes or erroneous assumptions in extrapolating bathymetric tracks to large areas could have overestimated the number of seamounts. In contrast, the criteria in this study are strictly visual. Seamounts with sonar-brightnesses similar to the surrounding seafloor should be virtually invisible on the *GLORIA* mosaic. Thus, this study may underestimate the number of seamounts.

The relative lack of and small size of seamounts near the Murray and Molokai FZ's (Figs. 1 and 9b, c) is inconsistent with other areas of the Pacific where this has been studied. Based on their analysis of the distribution of seamounts near the EPR on the Cocos Plate, Batiza and Vanko (1983) proposed that magma ascent and seamount production are favored near fracture zones. However, Scheirer and Macdonald (1995) found that the heights and abundances of seamounts near EPR discontinuities are indistinguishable from those near mid-segments. A lack of seamounts near fracture zones might be caused by a reduction in magma supply or mantle upwelling near spreading axis discontinuities (Scheirer and Macdonald, 1995). Whether or not this applies to the HEEZ portion of the Murray and Molokai FZ's when they were near the ancestral EPR is uncertain. As discussed elsewhere in this paper, it is likely that some seamounts in the HEEZ formed after leaving

the EPR, making the interpretation of seamount distribution near the fracture zones somewhat ambiguous. At the very least, it is clear that fracture zones need not necessarily be loci for seamount production.

4.2. Dimensions

Diameters of the HEEZ seamounts are similar to those elsewhere in the Pacific. In both regions, abundance is inversely proportional to diameter as discussed previously in relation to Eq. (1). This is further illustrated in Fig. 10, where the fraction of seamounts as a function of diameter in the HEEZ is compared to seamounts near the EPR between 8° and 17°N (Scheirer and Macdonald, 1995) and on the Nazca Plate (Searle, 1983). In the case of the HEEZ and Nazca, the latter of which was also studied with *GLORIA*, the bin with the greatest abundance is 2–4 km. The bin with greatest abundance in the EPR study is between 4 and 6 km. In all three cases abundances decline fairly systematically away from the modal bin. The decline at lower sizes is likely due to resolution limitations.

The characteristic diameter (α^{-1}) of the HEEZ seamounts is 4.16 ± 0.11 km compared to 3.17 ± 0.4 km estimated for the whole Pacific (Jordan et al., 1983; Smith and Jordan, 1988). Converting the characteristic heights of Smith and Jordan (1988) to characteristic diameters by assuming a typical seamount aspect ratio of 0.1 (Smith, 1988) yields an α^{-1} of 2.57 ± 0.38 and 3.08 ± 0.67 km for their areas 1 and 2, respectively (Table 1). Area 1, between the Clarion and Murray FZ's, is tectonically analogous to the HEEZ regions between the Molokai and Murray FZ's and SE of the Molokai FZ, which have characteris-

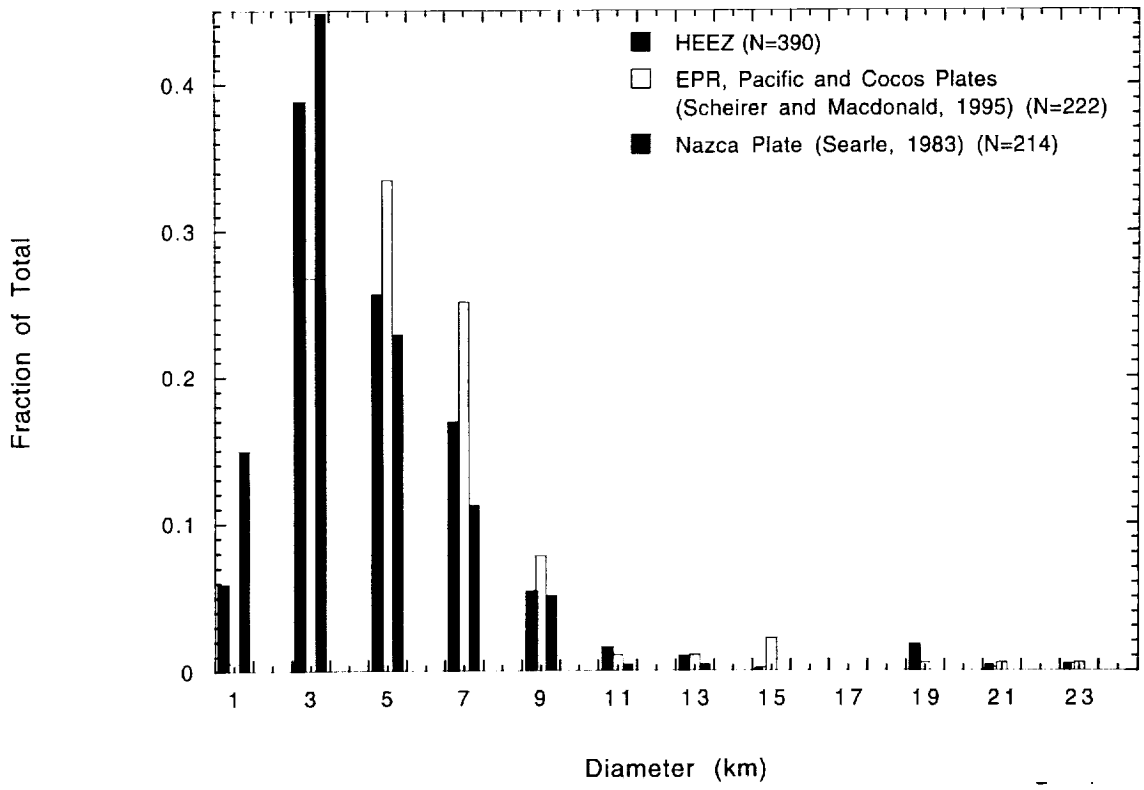

Fig. 10. Fractional abundance of other Pacific and HEEZ seamounts as a function of diameter. Diameters are binned for ±1 km from the value shown on the x-axis, the lower bound being inclusive and the upper exclusive.

tic diameters of 4.48 ± 0.13 and 4.88 ± 0.32 km, respectively. NW of the Murray FZ, α^{-1} is 17.7 ± 0.4 km, considerably greater than the value of 3.08 ± 0.67 km found in Smith and Jordan's area 2 (between the Murray and Mendocino FZ's). At face value, these statistics indicate that seamount abundance increases less with decreasing diameter in the HEEZ compared to analogous regions in the Pacific and the Pacific overall. This cannot be explained by thicker sediment in the HEEZ, because sediment deposition should uniformly lower diameters, decreasing the estimated number of seamounts of all sizes per unit area (v_0), but not altering the slope of the abundance–diameter distribution [$\exp(-\alpha D)$]. The relatively high characteristic diameters in the HEEZ are therefore indicative of either a lower seamount abundance compared to the rest of the Pacific or, as discussed previously, differences between the identification methods used in this study and that of Smith and Jordan (1988).

4.3. Morphology

The shapes of Pacific seamounts vary, and the nomenclature and classification schemes differ from author to author. Common categories are "cones", "truncated cones", "shields", and "flat-topped volcanoes". Guyots and some seamounts are commonly described as having "star" or "starfish" shapes. The classes of HEEZ seamounts identified here, the "cones", amorphous "heaps", "pancakes", and "stars" represent fairly well the range of seamount morphologies in the Pacific, both near the rise axis and in intraplate settings.

At the EPR, the range of seamount sizes increases with distance from the axis. Only small constructs are near the axis and an increasing number of larger ones are found farther away (Smith and Jordan, 1988; Scheirer and Macdonald, 1995). Similarly, morphology changes from mainly small conical and dome-shaped seamounts near the axis to an increasing abundance of irregular and polygonal volcanoes at greater distances to those with "upturned soup bowl" shapes (flat-topped with convex upward flanks) in the outermost regions (Fornari et al., 1984, 1987a). The small conical volcanoes probably are equivalent to the HEEZ cones and the dome-shaped volcanoes are similar to the heaps and some pancakes. The "upturned soup bowls" are closest to the HEEZ pancakes in morphology. If seamounts form close together, they may form volcanic ridges (Batiza, 1989), analogous to the "ridge mounds" identified here. If the seamounts are large, the development of flank rift zones may give them star-like shapes in planview like those seen here (although this morphology has mostly been attributed to guyots) (Batiza and Vanko, 1983; Vogt and Smoot, 1984; Batiza, 1989; Mammerickx, 1989).

Most seamounts in the Pacific Plate interior were formed near, then transported away from the EPR (Fornari et al., 1987b; Abers et al., 1988; Smith and Jordan, 1988; Smith, 1991). Thus, it is not surprising that the morphology of seamounts in intraplate settings is similar to that of seamounts near the spreading center. For example, the occurrence of dome and truncated cone shaped volcanoes within the Pacific Plate is common. Hollister et al. (1978) noted a concentration of the former in the Philippine Sea and the latter in the northwest Pacific. Searle (1983) found 214 intraplate seamounts greater than 1 km wide in *GLORIA* images of the Nazca Plate. Of the volcanoes more than 4 km in diameter, 70% consist of steep-sided (mean and maximum slopes of 18° and 36°, respectively), "truncated cones" with summit plateaus that are slightly concave upward.

Most of the secondary features of the HEEZ seamounts have been documented in other regions as well. Calderas or craters on seamounts are common in some regions (Searle, 1983; Fornari et al., 1984, 1987a). For example, Searle (1983) found that out of the 214 seamounts surveyed by *GLORIA* on the Nazca Plate, ~45% had "calderas" (defined as depressions greater than 1 km in diameter) or "craters" (<1 km wide). This compares to 17% found in this study. In contrast, summit depressions are completely lacking in other areas, such as the western Pacific and Philippine Basin at depths between 2000 and 5000 m (Hollister et al., 1978). The smaller mounds found on ~10% of the HEEZ seamounts (Figs. 2g and h) may in many cases be comparable to spine-like bulges that project through the sediment at other intra-plate Pacific volcanoes (e.g., Hollister et al.,

1978). Examples of coalesced seamounts (Figs. 2c and g) exist in other Pacific locales as well (Batiza and Vanko, 1983; Searle, 1983). Searle (1983) found that at least 4% of the seamounts imaged by *GLORIA* on the Nazca Plate have overlapping relations. This matches the 4% value found for the Hawaii EEZ. Features interpreted as landslides (Fig. 2h) may exist on other Pacific seamounts too (Searle, 1983). Normal faults on seamounts, such as those splitting some of the seamounts in the HEEZ (Fig. 2i), are also found on seamounts atop EPR-parallel faults and fissures (Fornari et al., 1987a; Edwards et al., 1991) and in intra-plate settings (Searle, 1983). However only one seamount graben, that striking NW–SE, has an orientation expected for extensional stresses caused by seafloor spreading or lithospheric flexure. To the best of this author's knowledge volcanoes that look like the HEEZ seamounts with truncated edges (Fig. 2b) have not been reported elsewhere, although this is not surprising considering their rarity in the HEEZ. Unfortunately, multibeam bathymetry and side-scan sonar from multiple angles needed to better characterize this enigmatic class of seamounts are unavailable.

5. Discussion

The similarity between the morphology and dimensions of HEEZ seamounts and those elsewhere in the Pacific suggests that their modes of formation were similar. Two end-member models have been proposed for the formation of seamounts at the EPR which account for the change in size and morphology of near-axis seamounts with distance from the axis (Fornari et al., 1984, 1987a; Smith and Jordan, 1988; Batiza, 1989; Scheirer and Macdonald, 1995): (1) all seamounts form near the axis and evolve as they are carried away by plate motion (Fornari et al., 1984, 1987a; Batiza, 1989; Scheirer and Macdonald, 1995), or (2) the time interval over which seamounts form is relatively short, so that their size and morphology are dependent on their distance from the rise (Barone and Ryan, 1990). The *GLORIA* data alone cannot determine which model is more applicable to the HEEZ seamounts.

However, the alignment of seamounts along trends parallel to the Necker Ridge and the high areal density of seamounts between the Murray and Molokai FZ's seen in the *GLORIA* images suggest that post-EPR igneous processes were not limited to the formation of some of the Musician seamounts (Pringle, 1993) or the large Pliocene–Pleistocene North Arch flow field (Clague et al., 1990). There are no discernible differences in morphology between these seamounts and those aligned with the fracture zones, which probably formed at the EPR. Thus, submarine volcanism in the plate interior seems capable of producing seamounts similar to those seen near spreading centers, regardless of the exact mechanism by which this occurs.

The question of to what extent intraplate seamount volcanism has occurred off-axis from the Hawaiian Ridge has important implications for the volcanic–tectonic history of the crust near Hawaii. Although this study documents the characteristics of HEEZ seamounts and strongly suggests that previously undocumented post-EPR seamounts exist, more definitive data are needed. Samples are sorely needed from these seamounts to find out if they derive from near the ancestral EPR or formed later. Geochemistry and ages must be determined. The limited sampling to date indicates that seamounts born near the EPR, including the Musicians, derive from a more depleted mantle source than volcanoes in the Hawaiian chain (Batiza and Vanko, 1984; Hess, 1989; Pringle, 1992, 1993; Pringle et al., 1990). The North Arch lavas also seem to derive from a relatively depleted mantle source but are more alkalic than the majority of Hawaiian lavas (Clague et al., 1990). Thus, geochemical analyses should help determine where the seamounts formed. A more unequivocal test of seamount origin is dating. Radiometric and paleomagnetic (for seamounts not formed during the Cretaceous quiet interval) ages can be determined for relatively unaltered samples. Thickness of sediment cover, thickness of weathering rinds, and dating of sediment in contact with the samples can also be used to estimate age. Dating of the seamounts will determine if the seamounts formed on the periphery of the EPR, near the Hawaiian

chain, or somewhere in between. Clearly, much important and exciting work remains.

Acknowledgements

Comments from two anonymous reviewers substantially improved this paper. Critiques of this work at intermediate stages by John Dvorak, George McGill, Daniel Sheirer, and Debbie Smith are much appreciated. This project began while I was an employee of the U.S. Geological Survey, Menlo Park, Californa. Jim Moore suggested this study and, with Bill Normark, supported my access to the *GLORIA* data. They provided guidance through the data collection stage of the project and reviewed preliminary versions of the manuscript. Chris Gutmacher and Michael Torresan made available raw bathymetry data and Tom Chase and Carolyn Degnan provided bathymetric maps. Debbie Smith helped with the statistical analyses and provided the computer code for determining statistical parameters. Conversations with Rodey Batiza and David Clague were very useful. Finally, this study would not have been possible without acquisition of the Hawaiian EEZ sidescan sonar data and for this I am grateful to the entire U.S. Geological Survey *GLORIA* team. Partial support was provided by NASA grant NAGW-4263 to the University of Massachusetts.

Appendix A

Listed are data for the seamounts in the HEEZ examined in this study. Longitudes and latitudes are shown to 0.1° although in some cases the accuracy is coarser. Diameters are the average of maximum and minimum widths.

ID	Lat. (°N)	Long. (°W)	Type	Secondary feature(s)	Ave. dia. (km)
NW of Murray:					
1	27.9	167.6	heap	crater(s)	8.8
2	27.7	167.8	heap	graben	7.5
3	27.3	168.0	heap	crater(s)	4.4
4	28.1	170.2	pancake		2.5
5	29.0	171.6	cone	summit mound	3.3
6	28.6	171.9	pancake	summit mound	5.7
7	28.6	172.0	pancake	coalesced, summit mound	8.8
8	28.5	172.3	heap		7.0
9	28.7	172.9	pancake		3.8
10	27.4	173.3	pancake		3.8
11	29.2	174.7	pancake	crater(s), truncated	4.3
12	29.4	174.8	pancake		3.6
13	29.1	174.9	heap	crater(s)	8.2
14	29.6	175.0	pancake		5.0
15	29.6	175.1	pancake		4.0
16	24.0	175.5	pancake		6.1
17	23.9	175.8	pancake		2.6
18	25.6	175.9	pancake		2.9
19	26.9	176.0	heap		18.3
20	29.6	176.2	pancake	summit mound	6.3
21	30.7	176.3	cone		5.3
22	30.6	176.3	heap		4.9
23	30.6	176.3	heap	coalesced	4.5
24	30.6	176.5	pancake		8.1
25	30.5	176.8	pancake		5.3

Appendix A (*continued*)

ID	Lat. (°N)	Long. (°W)	Type	Secondary feature(s)	Ave. dia. (km)
26	31.4	176.9	pancake		4.8
27	30.5	176.9	heap	crater(s)	4.8
28	30.7	177.1	pancake		4.5
29	31.3	177.1	pancake		3.5
30	31.3	177.1	pancake		5.9
31	30.5	177.2	heap		3.3
32	25.6	177.2	heap		19.4
33	32.0	177.4	cone		3.9
34	29.8	177.4	pancake		8.0
35	24.7	177.7	pancake		5.8
36	26.2	177.8	heap?		22.8
37	27.7	177.9	pancake	crater(s)	6.6
38	29.6	178.0	pancake		7.8
39	32.0	178.1	pancake	landslide	1.9
40	29.6	178.3	pancake	landslide, summit mound	4.8
41	27.0	178.4	pancake		4.9
42	31.0	178.5	pancake		1.7
43	26.8	178.7	pancake	crater(s), summit mound	4.4
44	25.5	179.0	pancake		3.4
45	30.7	179.1	pancake	summit mound	4.0
46	25.7	179.3	pancake	crater(s)	8.8
47	27.6	179.4	heap	crater(s), landslide	5.0
48	30.3	179.5	pancake		5.2
49	26.4	179.6	pancake	crater(s)	4.3
50	29.4	179.8	pancake	summit mound	4.1
51	25.9	179.8	heap		22.8
52	27.4	179.9	pancake	summit mound	6.3
53	27.5	180.0	pancake		1.9
54	25.4	180.0	pancake	summit mound	5.1
55	27.4	180.2	heap	summit mound	4.0
56	26.5	180.7	heap		4.8
57	28.3	180.8	pancake	crater(s)	3.0
58	26.0	180.9	pancake	coalesced	7.4
59	30.6	181.1	pancake	crater(s), summit mound	6.1
60	26.6	181.2	pancake	summit mound	7.5
61	27.1	181.2	pancake		6.9
62	29.9	181.6	pancake	summit mound	4.9
63	28.2	181.6	pancake		6.0
64	27.4	181.6	pancake		4.4
65	29.6	181.8	pancake	summit mound	7.8
66	28.0	182.0	heap	crater	29.7
67	27.7	182.0	pancake	crater(s), landslide	6.3
Between Murray and Molakai:					
68	23.3	154.0	heap	crater(s)	1.2
69	23.2	154.0	heap		2.6
70	23.3	154.0	heap		3.6
71	23.3	154.0	heap		2.7
72	23.3	154.1	heap		2.2
73	23.2	154.4	pancake		3.6
74	22.3	154.5	pancake	summit mound	4.4
75	23.1	154.5	pancake		2.5

Appendix A (*continued*)

ID	Lat. (°N)	Long. (°W)	Type	Secondary feature(s)	Ave. dia. (km)
76	23.3	154.7	heap		2.0
77	22.4	154.8	heap		7.6
78	22.5	155.0	heap		2.8
79	23.5	155.0	pancake	crater(s)	7.0
80	20.8	155.1	cone		2.1
81	22.6	155.1	pancake	crater(s)	6.6
82	20.6	155.2	pancake		3.1
83	23.5	155.2	heap		3.8
84	22.7	155.3	heap	crater(s)	7.2
85	23.4	155.4	heap		5.2
86	23.8	155.8	cone		3.8
87	23.9	155.9	pancake		3.3
88	23.7	155.9	cone		2.6
89	23.0	156.0	heap		7.8
90	23.7	156.0	cone		2.0
91	23.0	156.0	heap	landslide	7.8
92	23.3	156.6	cone		5.8
93	23.7	156.7	heap		4.0
94	23.4	156.7	cone		2.0
95	23.4	156.8	heap		2.0
96	23.4	156.8	heap		3.2
97	23.5	156.8	cone	crater(s)	5.8
98	23.4	156.8	cone	crater(s)	2.2
99	23.4	156.8	cone		2.6
100	24.4	156.8	heap		6.2
101	23.4	156.9	heap	summit mound	1.8
102	23.2	156.9	cone		2.8
103	23.2	156.9	cone		1.6
104	24.0	156.9	pancake	landslide	7.2
105	23.2	156.9	cone		2.0
106	23.2	156.9	cone		2.6
107	23.8	156.9	heap		6.8
108	23.3	157.0	cone		3.0
109	24.4	157.0	pancake		6.4
110	23.8	157.0	pancake		6.2
111	23.1	157.0	heap		3.4
112	23.8	157.1	heap		4.7
113	23.1	157.1	pancake		2.0
114	23.3	157.1	pancake		6.6
115	23.1	157.1	heap		3.2
116	23.2	157.2	pancake		5.2
117	23.6	157.2	pancake	crater(s)	4.4
118	24.9	157.6	heap	crater(s)	14.1
119	23.8	157.6	heap		3.4
120	23.9	157.6	heap	crater(s)	2.8
121	24.9	157.6	pancake		2.8
122	23.4	157.7	heap		4.4
123	23.4	157.7	pancake		4.8
124	24.6	157.8	heap	coalesced	7.6
125	24.7	157.9	heap		10.3
126	24.2	158.0	heap		3.6
127	24.2	158.0	heap		6.6
128	24.1	158.1	heap		7.2

Appendix A (*continued*)

ID	Lat. (°N)	Long. (°W)	Type	Secondary feature(s)	Ave. dia. (km)
129	24.6	158.1	pancake	summit mound	5.2
130	24.5	158.4	heap		3.6
131	24.5	158.4	cone		3.8
132	24.5	158.4	pancake	crater(s)	3.4
133	24.3	158.5	heap	landslide	4.4
134	24.5	158.6	cone		3.8
135	23.5	158.7	pancake		10.3
136	24.3	158.7	pancake		2.9
137	24.7	158.7	cone		4.0
138	23.7	158.8	heap		7.2
139	23.4	158.9	pancake	crater(s)	7.6
140	23.7	158.9	heap		2.5
141	23.6	158.9	pancake		3.8
142	23.5	158.9	pancake		4.4
143	24.7	158.9	pancake		4.0
144	25.2	159.1	heap		2.8
145	23.6	159.1	pancake	summit mound	4.2
146	23.7	159.1	heap	truncated	4.2
147	25.2	159.1	heap		3.8
148	23.8	159.2	heap	crater(s)	3.6
149	23.5	159.2	heap		4.5
150	23.6	159.2	pancake	summit mound	3.2
151	23.7	159.2	heap	coalesced	9.5
152	24.0	159.2	pancake	crater(s)	4.8
153	24.0	159.3	heap		5.0
154	24.1	159.3	pancake	crater(s)	4.4
155	24.1	159.3	heap		2.2
156	24.1	159.3	heap		2.2
157	24.1	159.4	heap		2.8
158	24.1	159.4	heap		3.8
159	24.1	159.4	heap		2.7
160	24.1	159.4	pancake		2.0
161	24.1	159.4	heap		4.2
162	24.1	159.4	pancake	summit mound	2.4
163	25.3	159.5	heap		1.8
164	24.0	159.5	heap		2.8
165	25.3	159.5	pancake		1.8
166	25.3	159.5	pancake		1.2
167	25.3	159.5	cone		2.0
168	23.7	159.6	pancake	coalesced	8.2
169	24.4	159.6	pancake		4.4
170	25.3	159.6	heap		4.2
171	25.2	159.6	cone		2.2
172	25.2	159.6	cone		2.4
173	25.2	159.7	cone		2.4
174	25.2	159.7	cone		1.3
175	25.2	159.7	cone		2.0
176	23.7	159.7	pancake	summit mound	6.0
177	25.1	159.7	pancake		3.0
178	24.1	159.7	pancake		4.2
179	25.3	159.7	pancake	coalesced	3.6
180	23.7	159.8	pancake	summit mound	5.6
181	24.5	159.9	heap		5.8

Appendix A (*continued*)

ID	Lat. (°N)	Long. (°W)	Type	Secondary feature(s)	Ave. dia. (km)
182	24.7	159.9	pancake		3.4
183	24.2	160.0	heap	coalesced	6.0
184	23.9	160.0	cone		2.4
185	23.7	160.0	pancake	summit mound	5.6
186	24.1	160.0	heap		2.2
187	24.1	160.0	cone		2.4
188	23.9	160.0	heap		2.2
189	23.9	160.0	cone		1.6
190	24.6	160.0	heap		2.4
191	24.2	160.1	pancake	coalesced	2.8
192	24.2	160.1	cone		2.2
193	24.2	160.1	heap	summit mound	7.2
194	24.6	160.1	heap		2.8
195	23.9	160.1	pancake		1.4
196	24.6	160.1	heap		2.2
197	23.9	160.1	pancake		5.1
198	24.2	160.1	heap		4.0
199	23.6	160.2	pancake		5.6
200	24.3	160.2	heap	crater(s)	2.0
201	24.1	160.2	cone		2.2
202	24.2	160.2	heap		2.4
203	24.9	160.2	pancake	crater(s)	4.4
204	24.1	160.3	pancake		3.6
205	24.1	160.3	pancake	summit mound	7.0
206	23.8	160.3	heap	crater(s)	8.2
207	24.8	160.5	pancake		4.0
208	24.8	160.5	pancake		4.0
209	24.0	160.6	heap	crater(s)	4.3
210	23.8	160.7	pancake		5.5
211	25.2	160.7	pancake	crater(s), truncated	4.3
212	25.5	160.7	pancake		3.6
213	23.8	160.8	heap	crater(s)	10.5
214	25.4	160.8	pancake		1.5
215	26.1	160.8	pancake	crater(s)	2.2
216	19.4	160.9	pancake	crater(s)	3.9
217	24.7	160.9	pancake	truncated	7.0
218	25.2	160.9	pancake		6.9
219	25.5	161.0	pancake	summit mound	1.7
220	24.8	161.1	pancake		6.2
221	25.3	161.2	pancake	graben	6.9
222	26.1	161.2	pancake		2.6
223	26.5	161.8	pancake		3.3
224	24.6	161.8	pancake		9.3
225 (Mendelssohn)	25.1	161.9	ridge mound		57.0
226	24.6	162.0	pancake		4.1
227	26.7	162.2	pancake		4.3
228	24.6	162.3	pancake		7.3
229	24.3	162.3	pancake		6.3
230	24.3	162.3	pancake		6.6
231	20.1	162.4	cone		2.2
232	19.0	162.4	pancake	crater(s)	7.2
233	26.5	162.4	pancake		3.1
234	21.1	162.6	pancake		4.2

Appendix A (*continued*)

ID	Lat. (°N)	Long. (°W)	Type	Secondary feature(s)	Ave. dia. (km)
235	21.5	162.7	heap?		12.6
236	21.4	162.8	heap?		18.2
237	21.8	162.8	star		12.6
238	22.3	162.9	star		18.2
239	21.1	163.1	heap?		13.7
240	22.5	163.2	star		19.4
241	21.5	163.2	pancake		8.9
242	21.6	163.3	pancake	summit mound	8.9
243	25.2	163.4	pancake	crater(s)	5.9
244	22.7	163.5	star		11.4
245	21.1	163.6	pancake	truncated	6.8
246	21.5	163.8	heap	crater(s), summit mound	6.1
247	21.5	163.8	pancake	crater(s), summit mound	6.4
248	20.9	164.0	pancake		5.0
249	20.9	164.1	pancake		6.4
250	24.5	164.1	pancake	crater(s), summit mound	5.2
251	24.9	164.3	heap	summit mound	4.5
252	25.8	164.3	pancake		2.9
253	25.3	164.3	pancake		5.9
254	24.9	164.5	pancake	crater(s), truncated	8.8
255	25.5	164.6	pancake		2.8
256	25.3	164.6	pancake	coalesced	5.8
257	25.3	164.6	pancake	coalesced	5.9
258	25.1	164.7	pancake		5.3
259	21.9	164.9	heap	landslide	2.8
260	21.5	165.0	pancake	crater(s)	6.6
261	25.0	165.0	pancake	graben	2.9
262	26.6	165.0	pancake	coalesced	3.4
263	26.7	165.1	pancake	coalesced	3.6
264	26.6	165.3	pancake	crater(s)	3.1
265	21.8	165.4	pancake	summit mound	3.1
266	26.3	165.4	heap		2.3
267	22.4	166.0	heap	crater(s)	4.9
268	20.5	166.0	heap	crater(s)	4.5
269	20.9	166.0	heap	summit mound	7.0
270	22.2	166.1	heap		6.5
271	20.9	166.2	pancake	crater(s)	7.6
272	22.1	166.2	pancake	crater(s)	6.4
273	21.5	166.3	pancake	truncated	3.0
274	22.3	166.3	pancake		5.5
275	27.0	166.3	pancake	crater(s)	3.5
276	22.1	166.3	heap		5.8
277	21.5	166.3	pancake		5.5
278	22.0	166.6	pancake		9.3
279	26.8	166.6	pancake	crater(s)	7.6
280	22.1	166.7	pancake		7.5
281	22.9	167.0	pancake	crater(s)	6.3
282	21.6	167.0	pancake		3.9
283	21.8	167.1	pancake		9.5
284	20.4	167.2	pancake		2.5
285	21.4	167.3	pancake		4.3
286	23.1	167.5	pancake		6.5
287	22.8	167.5	pancake		3.3

Appendix A (*continued*)

ID	Lat. (°N)	Long. (°W)	Type	Secondary feature(s)	Ave. dia. (km)
288	22.3	167.9	pancake		3.6
289	22.2	168.0	pancake		4.7
290	22.7	168.1	pancake		1.6
291	24.0	168.1	pancake		1.9
292	21.0	168.1	pancake		4.9
293	22.2	168.1	pancake		2.4
294	22.3	168.2	pancake		2.6
295	23.0	168.4	pancake		8.4
296	22.2	168.5	pancake		3.8
297	22.2	168.6	pancake		2.6
298	22.8	168.7	pancake	truncated	6.3
299	22.8	168.9	pancake	coalesced	4.8
300	22.6	169.0	pancake		3.4
301	22.8	169.0	pancake	coalesced	6.0
302	23.1	169.4	pancake		9.3
303	22.8	169.5	pancake	summit mound	8.1
304	22.0	169.5	pancake	coalesced	6.1
305	22.0	169.5	pancake	coalesced	7.6
306	21.8	169.7	pancake	landslide	7.3
307	22.0	169.9	pancake		8.3
308	21.9	170.0	pancake		7.6
309	22.2	170.3	pancake		8.9
310	21.8	170.4	pancake		6.8
311	22.4	172.5	pancake		6.8
312	22.2	172.7	pancake		4.4
313	22.4	172.7	pancake		6.4
314	23.3	173.8	pancake	crater(s)	1.8
315	23.6	173.8	pancake	truncated	5.8
316	23.3	174.6	heap		5.5
317	23.1	174.9	heap	crater(s)	9.5
SE of Molakai:					
318	19.6	151.8	pancake	crater(s)	3.3
319	18.4	151.9	pancake		7.0
320	21.3	152.0	pancake		4.0
321	20.8	152.0	pancake		3.2
322	20.9	152.1	heap	crater(s)	2.4
323	18.6	152.9	pancake		3.4
324	17.8	152.9	heap	crater(s)	3.0
325	18.8	153.0	cone		2.0
326	20.9	153.2	pancake	crater(s)	4.4
327	18.7	153.3	pancake		3.2
328	19.5	153.4	pancake	summit mound	5.9
329	18.3	153.4	pancake	summit mound	3.8
330	19.0	153.4	heap		1.6
331	19.0	153.4	heap		2.5
332	19.0	153.4	heap		1.6
333	19.0	153.4	heap	crater(s)	2.2
334	18.7	153.4	heap	summit mound	3.7
335	19.0	153.5	heap		1.4
336	19.0	153.5	heap		1.4
337	19.0	153.6	heap		2.6

Appendix A (*continued*)

ID	Lat. (°N)	Long. (°W)	Type	Secondary feature(s)	Ave. dia. (km)
338	19.0	153.6	heap		16.0
339	20.7	153.7	pancake	crater(s)	4.6
340	20.6	153.7	pancake		5.8
341	19.1	153.8	heap		36.5
342	19.2	154.0	pancake		3.2
343	17.1	154.1	pancake		4.7
344	19.4	154.2	heap		18.2
345	20.1	154.2	cone		5.9
346	16.8	154.3	pancake	crater(s)	3.0
347	16.8	154.4	pancake		2.4
348	21.1	154.4	heap		2.1
349	20.2	154.4	pancake		2.8
350	21.1	154.4	pancake		2.0
351	16.7	154.4	heap	summit mound	2.5
352	16.8	154.5	heap		2.1
353	16.8	154.5	heap		3.6
354	16.9	154.5	heap		2.9
355	16.7	154.5	pancake		3.0
356	16.9	154.5	heap		2.4
357	21.0	154.5	pancake		3.0
358	16.9	154.5	heap	crater(s)	2.3
359	16.7	154.6	pancake		2.4
360	16.2	154.6	pancake		5.0
361	17.6	154.6	heap		3.4
362	17.6	154.7	pancake		4.8
363	18.6	154.7	pancake	summit mound	2.4
364	17.6	154.7	pancake		4.8
365	16.1	154.7	heap		5.4
366	16.4	155.4	pancake		10.1
367	16.3	155.5	pancake		5.8
368	16.7	156.0	heap		3.2
369	16.6	156.1	heap	summit mound	3.2
370	16.7	156.1	heap		2.4
371	15.8	156.1	cone		2.3
372	16.0	156.4	pancake		1.6
373	16.1	156.6	heap		13.9
374	16.1	156.6	heap		9.4
375	18.7	156.9	heap		34.2
376 (Jaggar)	19.3	156.9	ridge mound?		27.4
377	16.3	157.0	heap		10.4
378	16.3	157.1	cone		2.4
379 (Pensacola)	18.3	157.2	star		18.3
380	15.7	157.2	cone		1.4
381	15.9	157.6	pancake		2.0
382	15.9	157.6	cone		2.4
383	17.4	157.8	heap	summit mound	2.4
384	17.0	157.9	pancake		3.6
385 (Cross)	18.7	158.1	star?		25.3
386 (Brigham)	19.1	158.6	ridge mound?		20.6
387 (Bishop)	18.8	159.0	heap?		25.1
388	19.8	159.2	pancake	summit mound	5.2
389	19.8	159.3	pancake	crater(s)	2.6
390	18.6	160.0	pancake		4.2

References

Abers, G.A., Parsons, B., Weissel, J.K., 1988. Seamount abundances and distributions in the southeast Pacific. Earth Planet. Sci. Lett. 87, 137–151.

Atwater, T., Severinghaus, J., 1988. Tectonic map of the north central Pacific Ocean. In: The Eastern Pacific Ocean and Hawaii, Vol. N of the Geology of North America. Geol. Soc. Am., Boulder, CO.

Barone, A.M., Ryan, W.B.F., 1990. Single plume model for asynchronous formation of the Lamont seamounts and adjacent East Pacific Rise terrains. J. Geophys. Res. 95, 10,801–10,827.

Batiza, R., 1982. Abundances, distribution, and sizes of volcanoes in the Pacific Ocean and implications for the origin of non-hotspot volcanoes.. Earth Planet. Sci. Lett. 60, 195–206.

Batiza, R., 1989. Seamounts and seamount chains of the Eastern Pacific. In: Winterer, E.L., Hussong, D.M., Decker, R.W. (Eds.), The Eastern Pacific Ocean and Hawaii, Vol. N. of The Geology of North America. Geol. Soc. Am., Boulder, CO, pp. 289–306.

Batiza, R., Vanko, D., 1983. Volcanic development of small oceanic central volcanoes on the flanks of the East Pacific Rise inferred from narrow-beam echo-sounder surveys. Mar. Geol. 54, 53–90.

Batiza, R., Vanko, D., 1984. Petrology of young Pacific seamounts. J. Geophys. Res. 89, 11,235–11,260.

Bemis, K.G., Smith, D.K., 1993. Production of small volcanoes in the Superswell region of the South Pacific. Earth Planet. Sci. Lett. 118, 251–262.

Cailleux, A., 1975. Frequence des monts sous-marins dans trois parties des océans pacifique et indien. Cah. Géogr. Qué. 19, 553.

Chase, T.E., Young, J.D., Degnan, C.H., Lucky, H.E.R., Riordan, J.A., Webber, L.D., 1992. Marine topography of offshore Hawaiian islands. In house U.S. Geol. Surv. Map Ser.

Clague, D.A., Dalrymple, G.B., 1989. The Hawaiian Emperor volcanic chain, Part 1: Geologic evolution. In: Decker, R.W., Wright, T.L., Stauffer P.H. (Eds.), Volcanism in Hawaii, Vol. 1. U.S. Geol. Surv., Prof. Pap. 1350, 5–54 [also published as: Clague, D.A., Dalrymple, G.B., 1987. Tectonics, geochronology, and origin of the Hawaiian Emperor volcanic chain. In: Winterer, E.L., Hussong, D.M., Decker, R.W. (Eds.), The Eastern Pacific Ocean and Hawaii, Vol. N of The Geology of North America. Geol. Soc. Am., Boulder, CO, pp. 188–217].

Clague, D.A., Holcomb, R.T., Sinton, J.M., Detrick, R.S., Torresan, M.E., 1990. Pliocene and Pleistocene alkalic flood basalts on the seafloor north of the Hawaiian Islands. Earth Planet. Sci. Lett. 98, 175–191.

Edwards, M.H., Fornari, D.J., Malinverno, A., Ryan, W.B.F., 1991. The regional tectonic fabric of the East Pacific Rise from 12°50′N to 15°10′N. J. Geophys. Res. 96, 7995–8017.

Fornari, D.J., Campbell, J.F., 1987. Submarine topography around the Hawaiian Islands. In: Decker, R.W., Wright, T.L., Stauffer, P.H. (Eds.), Volcanism in Hawaii, Vol. 1. U.S. Geol. Surv., Prof. Pap. 1350, 109–124.

Fornari, D.J., Ryan, W.B.F., Fox, P.J., 1984. The evolution of craters and calderas on young seamounts: Insights from Sea Marc I and Sea Beam sonar surveys of a small seamount group near the axis of the East Pacific Rise at ~10°N. J. Geophys. Res. 89, 11,069–11,083.

Fornari, D.J., Batiza, R., Allen, J.F., 1987a. Irregularly shaped seamounts near the East Pacific Rise: Implications for seamount origin and rise axis processes. In: Keating, B.H., Fryer, B., Batiza, R., Boehlert, G.W. (Eds.), Seamounts, Islands, and Atolls. Am. Geophys. Union, Washington, DC, pp. 35–47.

Fornari, D.J., Batiza, R., Luckman, M.A., 1987b. Seamount abundances and distribution near the East Pacific Rise 0–24°N based on seabeam data. In: Keating, B.H., Fryer, B., Batiza, R., Boehlert, G.W. (Eds.), Seamounts, Islands, and Atolls. Am. Geophys. Union, Washington, DC, pp. 13–21.

Gardner, J., 1992. The face of the U.S. seafloor. U.S. Geol. Surv., Public Iss. Energy Mar. Geol., 2 pp.

Geyer, R.A. (Ed.), 1992. CRC Handbook of Geophysical Exploration at Sea, Hard Minerals, 2nd ed. CRC Press, Boca Raton, FL, 86 pp.

Hess, P.C., 1989. Origins of Igneous Rocks. Harvard University Press, Cambridge, MA, 336 pp.

Hollister, C.D., Glenn, M.F., Lonsdale, P.F., 1978. Morphology of seamounts in the Western Pacific and Philippine Basin from multi-beam sonar data. Earth Planet. Sci. Lett. 41, 405–418.

Hull, D.M., 1993. 1. Quaternary, Eocene, and Cretaceous radiolarians from the Hawaiian Arch, northern Equatorial Pacific Ocean. In: Dearmont, L.H., Marin, J.A. (Eds.), Proceedings of the Ocean Drilling Program, Scientific Results, Vol. 136. Ocean Drill. Prog., College Station, TX, pp. 3–25.

Jordan, T.H., Menard, H.W., Smith, D.K., 1983. Density and size distribution of seamounts in the Eastern Pacific inferred from wide-beam sounding data. J. Geophys. Res. 88, 10,508–10,518.

Lonsdale, P.F., 1985. Nontransform offsets of the Pacific–Cocos Plate boundary and their traces on the rise flank. Geol. Soc. Am. Bull. 96, 313–327.

Macdonald, K.C., 1989. Tectonic and magmatic processes on the East Pacific Rise. In: Winterer, E.L., Hussong, D.M., Decker, R.W. (Eds.), The Eastern Pacific Ocean and Hawaii, Vol. N. of The Geology of North America. Geol. Soc. Am., Boulder, CO, pp. 93–110.

Macdonald, K.C., Sempere, J.-C., Fox, P.J., 1984. East Pacific Rise from Siqueiros to Orozco fracture zones: Along-strike continuity of axial neovolcanic zones and structure and evolution of overlapping spreading centers. J. Geophys. Res. 89, 6049–6069.

Mammerickx, J., 1989. Large-scale undersea features of the Northeast Pacific. In: Winterer, E.L., Hussong, D.M., Decker, R.W. (Eds.), The Eastern Pacific Ocean and Hawaii, Vol. N of The Geology of North America. Geol. Soc. Am., Boulder, CO, pp. 5–14.

Menard, H.W., 1959. Geology of the Pacific seafloor. Experimentia 15, 205–213.

Moore, J.G., 1987. Subsidence of the Hawaiian Ridge. In: Decker, R.W., Wright, T.L., Stauffer, P.H. (Eds.), Volcanism in Hawaii, Vol. 1, U.S. Geol. Surv., Prof. Pap. 1350, 85–100.

Moore, J.G., Clague, D.A., Holcomb, R.T., Lipman, P.W., Normark, W.R., Torresan, M.E., 1989. Prodigious submarine landslides on the Hawaiian Ridge. J. Geophys. Res. 94, 17,465–17,484.

Moore, J.G., Normark, W.R., Holcomb, R.T., 1994. Giant Hawaiian landslides. Annu. Rev. Earth Planet. Sci. 22, 119–144.

Phipps Morgan, J., Morgan, W.J., Price, E., 1995. Hotspot melting generates both hotspot volcanism and a hotspot swell? J. Geophys. Res. 100, 8045–8062.

Pringle, M.S., 1992. Geochronology and petrology of the Musicians seamounts, and the search for hot spot volcanism in the Cretaceous Pacific. Ph.D. dissertation, University of Hawaii, Honolulu, HI, 235 pp.

Pringle, M.S., 1993. Age progressive volcanism in the Musicians seamounts: A test of the hot spot hypothesis for Late Cretaceous Pacific. In: The Mesozoic Pacific: Geology, Tectonics, and Volcanism. Am. Geophys. Union, Geophys. Monogr. 77, 187–215.

Pringle, M.S., Sinton, J.M., Staudigel, H., 1990. Petrology of the Musicians and S. Hawaiian seamounts: Anomalous near-ridge seamount volcanism. Trans. Am. Geophys. Union 71, 1667.

Scheirer, D.S., Macdonald, K.C., 1995. Near-axis seamounts on the flanks of the East Pacific Rise. J. Geophys. Res. 100, 2239–2259.

Searle, R.C., 1983. Submarine central volcanoes on the Nazca Plate — High-resolution sonar observations. Mar. Geol. 53, 77–102.

Smith, D.K., 1988. Shape analysis of Pacific seamounts. Earth Planet. Sci. Lett. 90, 457–466.

Smith, D.K., 1991. Seamount abundances and size distributions, and their geographic variations. Rev. Aquat. Sci. 5, 197–210.

Smith, D.K., Jordan, T.H., 1988. Seamount statistics in the Pacific Ocean. J. Geophys. Res. 93, 2899–2918.

Udistsev, G.B., Agapova, G.V., Larina, N.I., Marova, N.A., 1976. Seamounts of the Pacific Ocean — General features of relief of Pacific Ocean floor. In: Aoki, H., Lizuka, S. (Eds.), Volcanoes and Tectonosphere. Tokai University Press, Tokyo.

Vogt, P.R., Smoot, N.C., 1984. The Geisha guyots: Multibeam bathymetry and morphometric interpretation. J. Geophys. Res. 89, 11,085–11,107.

Wessel, P., 1993. A reeaximination of the flexural deformation beneath Hawaiian Islands. J. Geophys. Res. 98, 12,177–12,190.

Wessel, P., Keating, B.H., 1993. Temporal variations of flexural deformation in Hawaii. J. Geophys. Res. 98, 2747–2756.

Winterer, E.L., 1989. Sediment thickness map of the Northeast Pacific. In: Winterer, E.L., Hussong, D.M., Decker, R.W. (Eds.), The Eastern Pacific Ocean and Hawaii, Vol. N of The Geology of North America. Geol. Soc. Am., Boulder, CO, pp. 307–310.

Advertising information
Advertising orders and enquiries may be sent to: Elsevier Science, Advertising Department, The Boulevard, Langford Lane, Kidlington, Oxford, OX5 1GB, UK, tel.: (+44) (0) 1865 843565, fax: (+44) (0) 1865 843976. *In the USA and Canada:* Weston Media Associates, attn. Dan Lipner, P.O. Box 1110, Greens Farms, CT 06436-1110, USA, tel.: (203) 261 2500, fax: (203) 261 0101. *In Japan:* Elsevier Science Japan, Marketing Services, 1-9-15 Higashi Azabu, Minato-Ku, Tokyo 106, tel.: (+81) 3 5561 5033, fax: (+81) 3 5561 5047.

NOTE TO CONTRIBUTORS

A detailed Guide for Authors is available upon request. Please pay attention to the following notes:

Language
The official language of the journal is English.

Preparation of the text
a) The manuscript should preferably be prepared on a word processor and printed with double spacing and wide margins and include an abstract of not more than 500 words. **Also provide 4 to 6 keywords. These must be taken from the most recent edition of the AGI GeoRef Thesaurus and should be placed beneath the abstract.**
b) Authors should use IUGS terminology. The use of S.I. units is also recommended.
c) The title page should include the name(s) of the author(s), their affiliations, fax and e-mail numbers. In case of more than one author, please indicate to whom the correspondence should be addressed.

References
a) References in the text consist of the surname of the author(s), followed by the year of publication in parentheses. All references cited in the text should be given in the reference list and vice versa.
b) The reference list should be in alphabetical order.

Tables
Tables should be compiled on separate sheets and should be numbered according to their sequence in the text. Tables can also be sent as glossy prints to avoid errors in typesetting.

Illustrations
a) All illustrations should be numbered consecutively and referred to in the text.
b) Drawings should be lettered throughout, the size of the lettering being appropriate to that of the drawings, but taking into account the possible need for reduction in size. The page format of the journal should be considered in designing the drawings.
c) Photographs must be of good quality, printed on glossy paper.
d) Figure captions should be supplied on a separate sheet.
e) If contributors wish to have their original figures returned this should be requested in proof stage at the latest.
f) Colour figures can be accepted providing the reproduction costs are met by the author. Please consult the publisher for further information.

Page proofs
One set of page proofs will be sent to the corresponding author, to be checked for typesetting/editing. The author is not expected to make changes or corrections that constitute departures from the article in its accepted form. Proofs should be returned within 3 days. To avoid postal delay, authors are requested to return corrections to the desk-editor, Mr. Bernard Westerop, by FAX (+31.20.4852459) or e-mail (b.westerop@elsevier.nl).

Reprints
Fifty reprints of each article are supplied free of charge. Additional reprints can be ordered on a reprint order form which will be sent to the corresponding author upon receipt of the accepted article by the publisher.

Submission of manuscripts
a) All manuscripts should be submitted in triplicate to the Editorial Office *Marine Geology*, P.O. Box 1930, 1000 BX Amsterdam, The Netherlands.
b) Illustrations should also be submitted in triplicate. One set should be in a form ready for reproduction: the other two may be of lower quality.
c) Authors are requested to submit the names, addresses and telephone, facsimile and e-mail numbers of four potential referees with their manuscripts.
d) Letter-type contributions should be submitted in triplicate to the Editorial Office *Marine Geology, Letter Section*, P.O. Box 1930, 1000 BX Amsterdam, The Netherlands. Contributions for this section should not exceed 8 printed pages and should be complete in themselves. No foldout illustrations can be accepted. The manuscripts received will be published ca. *three months* after acceptance. In order to achieve rapid publication, no proofs will be sent to the authors. Manuscripts should therefore be prepared with the greatest possible care.
e) **The indication of a FAX and e-mail number on submission of the manuscript could assist in speeding communications. The FAX number for the Amsterdam office is: +31-20-4852696.**
f) Submission of an article is understood to imply that the article is original and unpublished and is not being considered for publication elsewhere.

Submission of electronic text
Authors are requested to submit the final text on a 3.5" or 5.25" diskette. It is essential that the name and version of the word processing program, the type of computer on which the text was prepared, and the format of the text files are clearly indicated.
Authors are requested to ensure that the contents of the diskette correspond exactly to the contents of the hard copy manuscript. Discrepancies can lead to proofs of the wrong version being made. The word processed text should be in single column format.
If available, electronic files of the figures should also be included on a separate floppy disk.

Authors in Japan please note: Upon request, Elsevier Science Japan will provide authors with a list of people who can check and improve the English of their paper (*before submission*). Please contact our Tokyo office: Elsevier Science Japan, 1-9-15 Higashi Azabu, Minato-ku, Tokyo 106, tel. (+81)-3-5561-5032, fax (+81)-3-5561-5045.

South Pacific Sedimentary Basins

Edited by **P.F. Ballance**

Sedimentary Basins of the World Volume 2

Sedimentary basins contain most of the extant record of the earth's history, and they provide us with most of our earth-sourced raw materials. Therefore their study is both scientifically and economically important. This book gives the first comprehensive coverage of sedimentary basins in the New Zealand region. Comprising 21 chapters by 32 authors, it discusses sedimentary basins ranging in age from Permian to Quaternary. The chapters are process- and topic-oriented. Three distinct basin-forming periods are covered:
1) Permian through Jurassic arc-related terranes;
2) Mid-Cretaceous through Oligocene extensional basins;
3) Neogene convergent margin basins.
Resource scientists investigating sedimentary basins and all researchers working on basin-related topics will find this volume of interest.

Contents: Introduction. List of Contributors. **PART A: Basins Related to Permian-to-Early Cretaceous Convergence on the Gondwana Margin.** 1. Geology and Geochemistry of the Caples Terrane, Otago, New Zealand: Compositional Variations near a Permo-Triassic Arc Margin (B.P. Roser *et al.*). 2. The Murihiku Arc-Related Basin of New Zealand (Triassic-Jurassic) (P.F. Ballance, J.D. Campbell). **PART B: Basins Related to Cretaceous-to-Paleogene Extension.** 3. Cretaceous Continental Rifts: New Zealand Region (M.G. Laird). 4. Sedimentary Evolution of the Bounty Trough: a Cretaceous Rift Basin, Southwestern Pacific Ocean. (L. Carter, R.M. Carter). 5. The Bounty Trough - Basement Structure Influences on Sedimentary Basin Evolution (B. Davy). 6. The Paleo-Pacific, Post-Subduction, Passive Margin Thermal Relaxation Sequence (Late Cretaceous-Paleogene) of the Drifting New Zealand Continent (P.F. Ballance). **PART C: Basins Related to Neogene Convergence.** 7. The Tempestuous 10 Million Year Life of a Double Arc and Intra-Arc Basin - New Zealand's Northland Basin in the Early Miocene (B.W. Hayward). 8. Volcano-Tectonic Controls on Sedimentation in the Taupo Volcanic Zone, New Zealand (R.C.M. Smith *et al.*). 9. The Tonga Frontal-Arc Basin (D.R. Tappin). 10. The New Zealand Neogene Forearc Basins (P.F. Ballance). 11. Southern Havre Trough-Bay of Plenty (New Zealand): Structure and Seismic Stratigraphy of an Active Back-Arc Basin Complex (I.C. Wright). 12. Crustal Dynamics Associated with the Formation of Wanganui Basin, New Zealand (T.A. Stern, G.M. Quinlan, W.E. Holt). 13. The Emerging, Imbricate Frontal Wedge of the Hikurangi Margin (K.B. Lewis, J.R. Pettinga). 14. Cenozoic Basins Adjacent to an Evolving Transform Plate Boundary, Southwest New Zealand (R.J. Norris, I.M. Turnbull). 15. A Subsiding Platform Adjacent to a Plate Boundary Transpression Zone: Neogene of Canterbury, New Zealand (B.D. Field, G.H. Browne). 16. Regression-Related Coal-Bearing Sequences in the Neogene of New Zealand: Relation to the Developing Alpine Fault Transform (P.J. Crosdale). 17. Hauraki Rift: A Young, Active, Intra-Continental Rift in a Back-Arc Setting (M.P. Hochstein, P.F. Ballance). **PART D: Individual Basins with Dual Histories: Cretaceous-to-Paleogene Extension Followed by Neogene Convergence.** 18. Cretaceous-Tertiary Sedimentation and Implied Tectonic Controls on the Structural Evolution of Taranaki Basin, New Zealand (J.A. Palmer, P.B. Andrews). 19. The Chatham Rise, New Zealand (R.A. Wood, R.H. Herzer). 20. The Challenger Plateau (R.A. Wood). 21. Depositional and Tectonic History of the Great South Basin (J.M. Beggs). **PART E: Summary.** 22. A Distant View of South Pacific Geology (K.J. Hsü). **References Index. Subject Index.**

1993 436 pages
Dfl. 345.00 (US $ 197.25)
ISBN 0-444-88287-1

ELSEVIER SCIENCE B.V.
P.O. Box 1930
1000 BX Amsterdam
The Netherlands

P.O. Box 945
Madison Square Station
New York, NY 10160-0757

The Dutch Guilder (Dfl.) prices quoted apply worldwide. US $ prices quoted may be subject to exchange rate fluctuations. Customers in the European Community should add the appropriate VAT rate applicable in their country to the price.

ELSEVIER SCIENCE B.V.